# Regioselective and Stereoselective Reactions of 2-Butyne Bound to a Resolved Chiral Tungsten(II) Center

Michael B. Wells,[†] Jonathan E. McConathy,[‡] Peter S. White,[‡] and Joseph L. Templeton*,[‡]

*Departments of Chemistry, University of North Carolina, Chapel Hill, North Carolina 27599-3290, and Campbell University, Buies Creek, North Carolina 27506*

*Received May 28, 2002*

Deprotonation of chiral complexes of the type Tp′(CO)(I)W{RC≡CCH$_2$R′} at the propargyl carbon followed by alkylation is regioselective and stereoselective. Photolysis liberates the elaborated alkynes from the metal complex. Resolution of metal diastereomers, with amido ligands, Tp′(CO)(NHR)W{CH$_3$C≡CCH$_3$} (NH$_2$R = ((*S*)-(−)-α-methylbenzylamine), has been accomplished by fractional crystallization. Conversion to an amine complex followed by iodide replacement of H$_2$NCHMePh produces separate enantiomers of Tp′(CO)(I)W{CH$_3$C≡CCH$_3$}. Methylation followed by benzylation of each enantiomer affords Tp′(CO)(I)W{CH$_3$C≡CCHMeCH$_2$Ph}. The alkynes (−)-CH$_3$C≡CCHMeCH$_2$Ph and (+)-CH$_3$C≡CCHMeCH$_2$Ph have been released from each of these enantiomerically enriched complexes in optically active form, as assayed by optical rotation and by $^1$H NMR with chiral shift reagents. The barrier to alkyne rotation in Tp′(CO)(I)W{RC≡CCH$_2$R′} complexes has been probed by variable-temperature $^1$H NMR, and extended Huckel molecular orbital calculations have been performed on model complexes. The origin of regioselectivity and stereoselectivity is considered in light of the X-ray structures of Tp′(CO)(I)W{CH$_3$C≡CCHMe(CH$_2$)$_4$I} (**7**) and Tp′(CO)(I)W{Me(PhCH$_2$)HCC≡CCHMeCH(OH)Ph} (**11**). The absolute configuration of Tp′(CO)W{CH$_3$C≡CCH$_3$}(NHCHMePh) (**(+)-14(*SS*)**) has been established by X-ray analysis with the resolving amine as reference.



## Introduction

Alkynes are useful in organic synthesis,[1] and accordingly, chiral alkynes are attractive for the synthesis of optically active compounds. Synthesis of alkynes by electrophilic addition to classical propargyl carbanion equivalents produces a mixture of allene and alkyne products because of the resonance relationship between the propargyl anion and the allenyl anion (Scheme 1).[2] Electrophilic addition has been directed to the propargyl carbon of lithio-1-(trimethylsilyl)propyne by the trimethylsilyl protecting group.[3]

Binding alkynes to transition metals activates and alters alkyne reactivity patterns. The relationship among alkyne, propargyl, and allenyl complexes has been the subject of a recent review.[4] Nucleophiles have been added regioselectively to cationic propargyl synthons, which were generated by binding an alkyne to a cobalt dimer.[5] Casey has reported regioselective and stereoselective hydride abstraction from the propargyl carbon of Cp*(CO)$_2$Re{RC≡CCH$_2$R′} to form cationic $\pi$ propargyl complexes.[6] Propargyl protons have been shown to be acidic in other metal alkyne complexes. Bergman and Watson demonstrated that the butyne methyl groups in [Cp(CO)Mo{CH$_3$C≡CCH$_3$}$_2$]$^+$ could be deuterated with triethylamine in deuterioacetone.[7] The nucleophilic properties of $\eta^2$-allenyl complexes prepared from [(Ph$_2$PCH$_2$CH$_2$PPh$_2$)(R$_2$NCS$_2$)(CO)W{MeOC≡CCH$_2$Ph}]$^+$ have been studied.[8] An $\eta^2$-allenyl complex has been isolated following deprotonation of [Cp(P(OMe)$_3$)$_2$Mo{PhC≡CCH$_2$Ph}]$^+$.[9]

**Scheme 1**

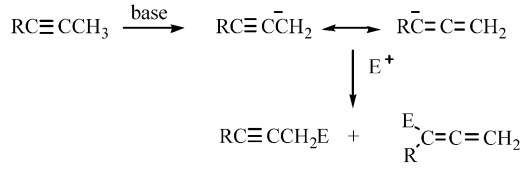


Deprotonation of chiral monomeric tungsten d$^4$ alkyne complexes of the type Tp′(CO)(I)W{PhC≡CCH$_2$R} (Chart 1) affords propargyl anion equivalents; formally these are $\eta^2$-allenyl complexes. Stereocontrol of electrophilic addition of alkyl halides and aldehydes to these prop-

[†] Campbell University.
[‡] University of North Carolina.

(1) (a) Stang, P. J., Diederich, F. Eds. *Modern Acetylene Chemistry*; VCH: New York, 1995. (b) Viehe, H. G., Ed. *Chemistry of Acetylenes*; Marcel Dekker: New York, 1969.
(2) Klein, J. In *The Chemistry of the Carbon−Carbon Triple Bond*; Patai, S., Ed.; Wiley: New York, 1978; Part I, pp 343−379.
(3) Corey, E. J.; Kirst, H. A.; Katzenellenbogen, J. A. *J. Am. Chem. Soc.* **1970**, *92*, 6314.
(4) Doherty, S.; Corrigan, J. F.; Carty, A. J.; Sappa, E. *Adv. Organomet. Chem.* **1995**, *37*, 39.
(5) Nicholas, K. M. *Acc. Chem. Res.* **1987**, *20*, 207.
(6) Casey, C. P.; Selmeczy, A. D.; Nash, J. R.; Yi, C. S.; Powell, D. R.; Hayashi, R. K. *J. Am. Chem. Soc.* **1996**, *118*, 6698.
(7) Watson, P. L.; Bergman, R. G. *J. Am. Chem. Soc.* **1980**, *102*, 2698.
(8) Gamble, A. S.; Birdwhistell, K. R.; Templeton, J. L. *J. Am. Chem. Soc.* **1990**, *112*, 1818.
(9) Feher, F. J.; Green, M.; Rodrigues, R. *J. Chem. Soc., Chem. Commun.* **1987**, 1206.

10.1021/om020416g CCC: $22.00 
Publication on Web 10/12/2002

**Chart 1**

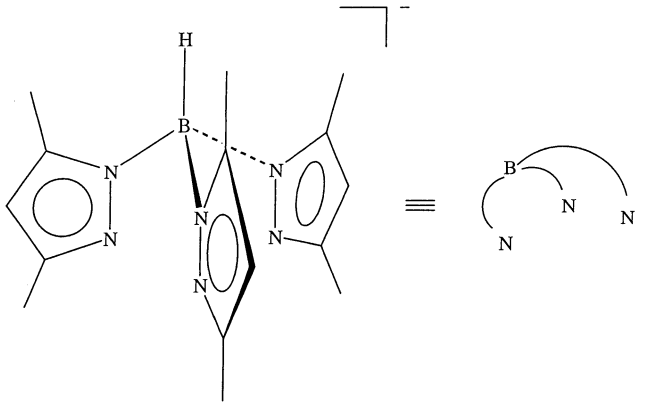

Tp' = hydridotris-(3,5-dimethylpyrazoyl) borate

**Scheme 2**

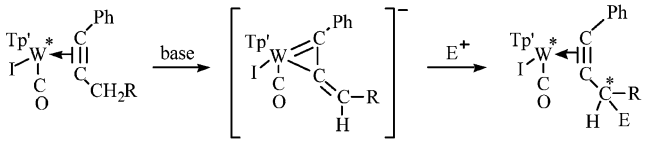

$\eta_2$-allenyl anion

argyl anion equivalents generated from coordinated 1-phenyl-1-propyne has been reported[10] (Scheme 2).

Enantioselective transformations have been achieved through the use of optically active transition-metal complexes.[11] Of course, optically resolved complexes are a prerequisite for enantioselective reactions. A procedure for resolution of the diastereomers of the amido complex Tp′(CO)(NHR)W{PhC≡$CCH_3$} (R = (*S*)-CHMePh) and subsequent conversion to yield multigram quantities of each enantiomer of Tp′(CO)(I)W{PhC≡$CCH_3$} has been developed.[12] Resolution of these complexes allows enantioselective elaboration of the complexed alkyne.

Once bound, removal of an intact alkyne from a transition metal is challenging.[13] Reported methods for alkyne removal include direct ligand substitution,[14] decomplexing by oxidizing or reducing the metal,[5] and other methods that compromise the carbon−carbon triple bond[15] such as removal of the alkyne as an olefin.[16] Alkyne complexes of the type Tp′(CO)(I)W{alkyne} resist alkyne loss by ligand substitution, and even oxidation and reduction fail to remove the intact alkyne from tungsten.[17]

Here, we report extension of alkyne derivatization that includes (1) regiocontrol of alkylation of symmetrical alkynes, (2) diastereoselective alkyne elaboration reactions of resolved metal complexes, and (3) isolation of optically enriched alkynes via photolytic cleavage of the metal−alkyne unit.

**Chart 2**

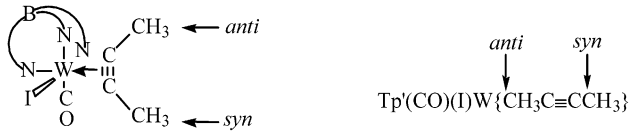

**Chart 3**

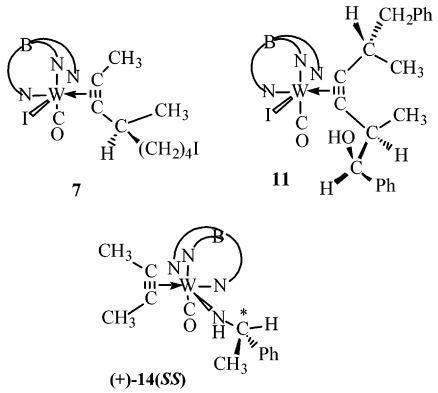

## Results and Discussion

Synthetic methods used to obtain this class of alkyne complexes are well established. A schematic representation of the 2-butyne complex defining syn and anti is shown in Chart 2.

The order of presentation below proceeds from discussion of key X-ray structures, through a consideration of barriers to isomerization, and on to alkyne decomplexation, before finally addressing reactions of the coordinated alkynes.

**X-ray Structures.** Single-crystal X-ray structures were obtained for Tp′(CO)(I)W{$CH_3$C≡CCHMe$(CH_2)_4$I} (**7**) and Tp′(CO)(I)W{Me(Ph$CH_2$)HCC≡CCHMeCH(OH)Ph} (**11**), to provide information about the regioselectivity and stereoselectivity of alkyne elaboration, and (+)-Tp′(CO)W{$CH_3$C≡$CCH_3$}(NHCHMePh) (**(+)-14(*SS*)**)- to establish the absolute configuration at the metal center (Chart 3).

An octahedral coordination sphere with the Tp′ ligand occupying three facial sites is revealed for **7**, **11**, and **(+)-14(*SS*)** (Figures 1−3). Data collection parameters



(10) Collins, M. A.; Feng, S. G.; White, P. S.; Templeton, J. L. *J. Am. Chem. Soc.* **1992**, *114*, 3771.
(11) (a) Brunner, H. *Adv. Organomet. Chem.* **1980**, *18*, 151. (b) Liebeskind, L. S.; Welker, M. E.; Fengl, R. W. *J. Am. Chem. Soc.* **1986**, *108*, 6328. (c) Seeman, J. I.; Davies, S. G. *J. Am. Chem. Soc.* **1985**, *107*, 6522. (d) Davies, S. G.; Walker, J. C. *J. Chem. Soc., Chem. Commun.* **1985**, 209. (e) Davies, S. G.; Easton, R. J. C.; Walker, J. C.; Warner, P. *J. Organomet. Chem.* **1985**, *296*, C40. (f) Ambler, P. W.; Davies, S. G. *Tetrahedron Lett.* **1985**, *26*, 2129. (g) Brookhart, M. S.; Studabaker, W. B. *Chem. Rev.* **1987**, *87*, 411. (h) Brookhart, M. S.; Liu, Y.; Goldman, E. W.; Timmers, D. A.; Williams, G. D. *J. Am. Chem. Soc.* **1991**, *113*, 927. (i) Bodner, G. S.; Fernandez, J. M.; Arif, A. M.; Gladysz, J. A. *J. Am. Chem. Soc.* **1988**, *110*, 4082. (j) Fernandez, J. M.; Emerson, K.; Larsen, R. D.; Gladysz, J. A. *J. Am. Chem. Soc.* **1986**, *108*, 8268. (k) Heah, P. C.; Patton, A. T.; Gladysz, J. A. *J. Am. Chem. Soc.* **1986**, *108*, 1185. (l) Garner, C. M.; Mendez, N. Q.; Kowalczyk, J. J.; Fernandez, J. M.; Emerson, K.; Larsen, R. D.; Gladysz, J. A. *J. Am. Chem. Soc.* **1990**, *112*, 5146. (m) Faller, J. W.; John, J. A.; Mazzieri, M. R. *Tetrahedron Lett.* **1989**, *30*, 1769.
(12) Caldarelli, J. L.; White, P. S.; Templeton, J. L. *J. Am. Chem. Soc.* **1992**, *114*, 10097.
(13) Templeton, J. L. *Adv. Organomet. Chem.* **1989**, *29*, 1.
(14) (a) Allen, S. R.; Baker, P. K.; Barnes, S. G.; Green, M.; Trollope, L.; Muir, L. M.; Muir, K. W. *J. Chem. Soc., Dalton Trans.* **1981**, 873. (b) Davidson, J. L.; Vasapollo, G. *J. Chem. Soc., Dalton Trans.* **1985**, 2239. (c) Herrick, R. S.; Leazer, D. M.; Templeton, J. L. *Organometallics* **1983**, *2*, 834.
(15) Giandomenico, C. M.; Lam, C. T., Lippard, S. J. *J. Am. Chem. Soc.* **1982**, *104*, 1263.
(16) (a) Thomas, J. L. *J. Am. Chem. Soc.* **1973**, *95*, 1838. (b) Thomas, J. L. *Inorg. Chem.* **1978**, *17*, 1507. (c) McDonald, J. W.; Corbin, J. L.; Newton, W. E. *J. Am. Chem. Soc.* **1975**, *97*, 1970. (d) Kamata, M.; Yoshida, T.; Otsuka, S.; Hirotsu, K.; Higuchi, T.; Kido, M.; Tatsumi, K.; Hoffman, R. *Organometallics* **1982**, *1*, 227.
(17) Wells, M. B.; Philipp, C. C.; Templeton, J. L. Unpublished results.

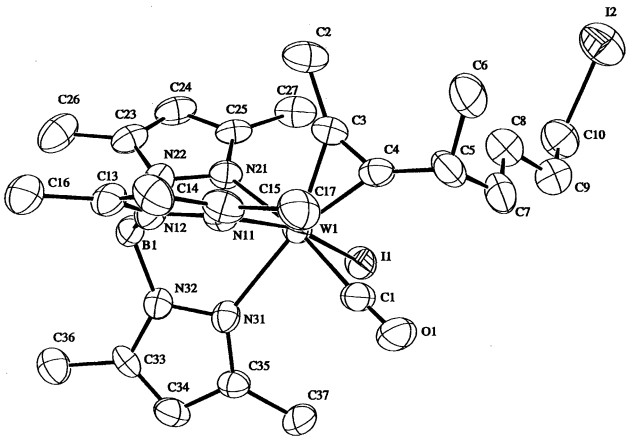


**Figure 1.** ORTEP of Tp′(CO)(I)W{$CH_3C{\equiv}CCHMe(CH_2)_4I$} (**7**).

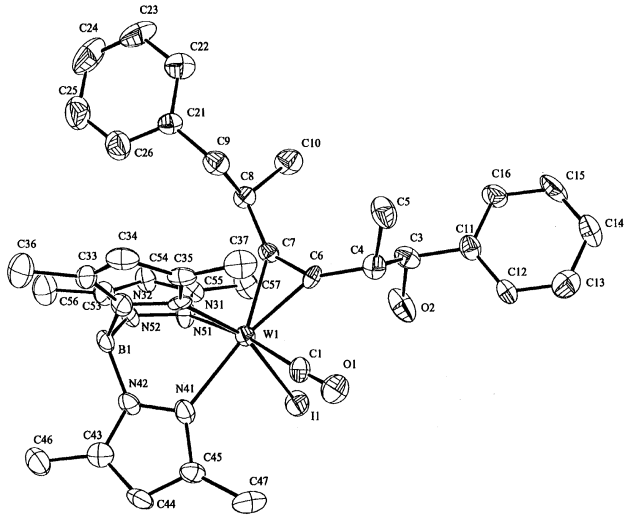


**Figure 2.** ORTEP of Tp′(CO)(I)W{$Me(PhCH_2)HCC{\equiv}CCHMeCH(OH)Ph$} (**11**).

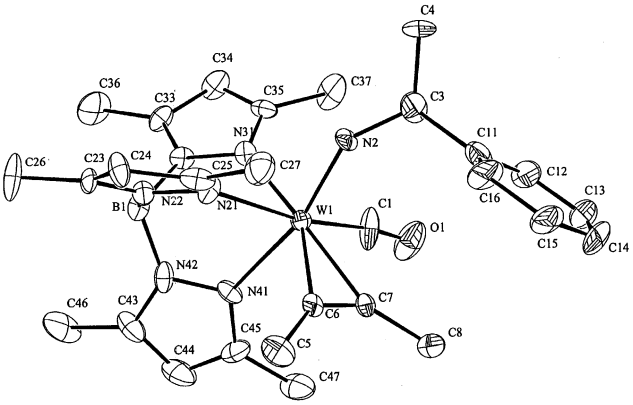


**Figure 3.** ORTEP of $S_WS_C$-(+)-Tp′(CO)W{$CH_3C{\equiv}CCH_3$}(NHCHMePh) (**(+)-14(*SS*)**).

are given in Table 1. Selected bond distances and bond angles for **7**, **11**, and **(+)-14(*SS*)** are reported in Tables 2−4, respectively.

In all three structures the alkyne is oriented along the W−CO axis, as is typical for $d^4$ alkyne carbonyl complexes.[13] A molecular orbital diagram is shown in Figure 4. The filled $d_{xy}$ orbital can donate into both the empty $\pi_{||}$* orbital of the alkyne ligand and one of the empty $\pi$* orbitals of the carbonyl. This arrangement allows the filled $\pi_{\perp}$ orbital of the alkyne to donate into the empty tungsten $d_{xz}$ orbital. The octahedral Tp′(CO)(I)W{RC≡CR′} framework for **7** is nearly congruent with **11**.

The absolute configuration of tungsten in the optically pure amido complex **(+)-14(*SS*)** was determined to be *S* by inspection of the X-ray structure (Figure 3) using the Baird−Sloan modification of the Cahn−Ingold−Prelog priority rules with the *S* configuration of the chiral amido carbon as the reference.[18] The amido ligand is also aligned along the W−CO axis, resulting in competition of the filled p orbital on the nitrogen with the filled alkyne $\pi_{\perp}$ orbital for donation into the empty $d_{xz}$ orbital of tungsten, as shown in Figure 5. The structure of this amido complex is analogous to the structure of the related amido complex Tp′(CO)W{PhC≡$CCH_3$}(NHCHMeEt).[19]

**Assessment of Isomerization Barriers.** To achieve regiocontrol of alkyne elaboration, significant barriers to alkyne rotation and to rotation of the deprotonated alkyne are necessary. Likewise, stereoselectivity of electrophile addition requires the absence of enantioface interconversion on the reaction time scale in the intermediate $\eta^2$-allenyl anion complexes. Potential modes of isomerization here are rotation of the alkyne unit in the neutral complexes and rotation of the deprotonated alkyne unit and enantioface interconversion, i.e., rotation of the putative C=C unit, in the anionic $\eta^2$-allenyl complexes.

Variable-temperature $^1$H NMR was used to experimentally determine the barrier to alkyne rotation in Tp′(CO)(I)W{$CH_3C{\equiv}C(CH_2)_4I$} (**4**) and Tp′(CO)(I)W{$CH_3C{\equiv}CCH_3$} (**1**). Extended Hückel molecular orbital calculations (EHMO) were used to estimate the barrier to alkyne rotation on the model complex $[H_3(CO)(I)W\{HC{\equiv}CH\}]^{2-}$. In addition, the rotational barrier of the deprotonated alkyne unit of the $\eta^2$-allenyl anion complexes was estimated by EHMO calculations on the model complex $[H_3(CO)(I)W\{HC{\equiv}CCH_2\}]^{3-}$, and the barrier to enantioface interconversion of the $\eta^2$-allenyl anion was also estimated by EHMO calculations on this model complex.

**Variable-Temperature $^1$H NMR Experiments.** The alkyne rotational barrier in **4** was calculated from line broadening in the $^1$H NMR spectra to be 21 kcal/mol. Surprisingly, no significant line broadening occurred, even at 120 °C, in the $^1$H NMR spectra of the 2-butyne complex **1.** Perhaps the ground-state configuration of **1** is lower in energy than the ground-state configuration of **4**, owing to the differences in steric bulk of the $-(CH_2)_4I$ unit in **4** and $-CH_3$ unit in **1**. In other words, the larger $-(CH_2)_4I$ group may force the alkyne away from its preferred alignment along the W−CO axis so that the ground-state energy is higher and the resulting barrier to isomerization is smaller. These large barriers to alkyne rotation reflect the strong and specific $\pi$ interactions among tungsten, carbonyl, and alkyne (detailed in the discussion of the X-ray structures). Similar barriers have been observed in Tp′(CO)(I)W-

(18) (a) Stanley, K.; Baird, M. C. *J. Am. Chem. Soc.* **1975**, *97*, 6599. (b) Sloan, T. *Top. Stereochem.* **1981**, *12*, 1.
(19) Francisco, L. W.; White, P. S.; Templeton, J. L. *Organometallics* **1996**, *15*, 5127.

**Table 1. Crystallographic Data Collection Parameters for 7, 11, and (+)-14(*SS*)**

| | 7 | 11 | (+)-14(*SS*) |
|---|---|---|---|
| mol formula | $WC_{25}H_{37}N_6BOI_2$ | $WC_{36}H_{44}N_6BO_2I$ | $WC_{28}H_{38}N_7BO$ |
| fw | 886.07 | 914.34 | 683.31 |
| cryst dimens, mm | 0.45 × 0.22 × 0.13 | 0.25 × 0.25 × 0.18 | 0.40 × 0.35 × 0.25 |
| space group | $P2_1/c$ | $P\bar{1}$ | $P2_12_12_1$ |
| *a*, Å | 8.2982(21) | 9.7218(24) | 11.0528(11) |
| *b*, Å | 23.374(7) | 11.191(3) | 13.0871(3) |
| *c*, Å | 16.573(4) | 18.622(8) | 20.5984(16) |
| α, deg | | 82.04(3) | |
| *β*, deg | 103.838(22) | 83.23(3) | |
| *γ*, deg | | 64.440(19) | |
| *V*, Å$^3$ | 3121.2(15) | 1806.3(10) | 2979.6(5) |
| *Z* | 4 | 2 | 4 |
| calcd density, g/cm$^3$ | 1.886 | 1.681 | 1.523 |
| radiation (wavelength, Å) | Cu Kα (1.540 56) | Mo Kα (0.710 73) | Mo Kα (0.710 73) |
| monochromator | | graphite | |
| linear abs coeff, mm$^{-1}$ | 22.87 | 4.15 | 3.99 |
| scan type | | *θ*/2*θ* with profile analysis | |
| background | | 10% of scan width on both sides | |
| 2*θ* limits, deg | 120 | 46 | 50 |
| h,k,l ranges | −9 to +9, 0−26, 0−18 | −9 to +10, 0−12, −19 to +20 | −2 to +13,−15 to +15, −24 to +24 |
| total no. of rflns | 4636 | 5402 | 3761 |
| no. of data with $I = 2.5\sigma(I)$ | 3047 | 3538 | 2947 |
| *R*, % | 5.3 | 5.0 | 4.5 |
| $R_w$, % | 6.6 | 5.9 | 6.2 |
| GOF | 1.75 | 1.65 | 1.91 |
| no. of params | 326 | 424 | 344 |
| largest param shift/*σ* | 0.002 | 0.007 | 0.156 |

**Table 2. Selected Bond Distances (Å) and Bond Angles (deg) for Tp′(CO)(I)W{CH$_3$C≡CCHMe(CH$_2$)$_4$I} (7)**

| | | | |
|---|---|---|---|
| W(1)−C(1) | 1.98(2) | W(1)−N(31) | 2.27(1) |
| W(1)−C(3) | 2.03(1) | C(1)−O(1) | 1.11(2) |
| W(1)−C(4) | 2.06(2) | C(2)−C(3) | 1.50(2) |
| W(1)−I(1) | 2.79(2) | C(3)−C(4) | 1.29(2) |
| W(1)−N(11) | 2.18(1) | C(4)−C(5) | 1.49(2) |
| W(1)−N(21) | 2.25(1) | | |
| C(1)−W(1)−C(3) | 107.7(6) | C(4)−W(1)−N(31) | 158.1(5) |
| C(1)−W(1)−C(4) | 71.6(6) | I(1)−W(1)−N(11) | 165.7(3) |
| C(1)−W(1)−I(1) | 87.2(5) | I(1)−W(1)−N(21) | 87.3(3) |
| C(1)−W(1)−N(11) | 96.0(6) | I(1)−W(1)−N(31) | 88.7(3) |
| C(1)−W(1)−N(21) | 168.4(5) | N(11)−W(1)−N(21) | 86.9(4) |
| C(1)−W(1)−N(31) | 87.6(5) | N(11)−W(1)−N(31) | 77.6(4) |
| C(3)−W(1)−C(4) | 36.7(6) | N(21)−W(1)−N(31) | 82.1(4) |
| C(3)−W(1)−I(1) | 105.4(5) | W(1)−C(1)−O(1) | 176(1) |
| C(3)−W(1)−N(11) | 86.9(5) | W(1)−C(3)−C(2) | 141(1) |
| C(3)−W(1)−N(21) | 83.7(5) | W(1)−C(4)−C(5) | 151(1) |
| C(3)−W(1)−N(31) | 159.4(5) | C(2)−C(3)−C(4) | 145(1) |
| C(4)−W(1)−I(1) | 96.9(4) | C(3)−C(4)−C(5) | 139(1) |
| C(4)−W(1)−N(11) | 97.3(5) | C(6)−C(5)−C(7) | 113(1) |
| C(4)−W(1)−N(21) | 119.3(5) | | |

**Table 3. Selected Bond Distances (Å) and Bond Angles (deg) for Tp′(CO)(I)W{Me(PhCH$_2$)HCC≡CCHMeCH(OH)Ph} (11)**

| | | | |
|---|---|---|---|
| W(1)−C(1) | 1.95(2) | W(1)−N(51) | 2.26(1) |
| W(1)−C(6) | 2.07(1) | C(1)−O(1) | 1.16(2) |
| W(1)−C(7) | 2.02(1) | C(4)−C(6) | 1.50(2) |
| W(1)−I(1) | 2.80(1) | C(6)−C(7) | 1.30(2) |
| W(1)−N(31) | 2.19(1) | C(7)−C(8) | 1.52(2) |
| W(1)−N(41) | 2.24(1) | C(3)−O(2) | 1.43(2) |
| C(1)−W(1)−C(6) | 71.5(5) | I(1)−W(1)−N(31) | 161.0(3) |
| C(1)−W(1)−C(7) | 107.2(5) | I(1)−W(1)−N(41) | 85.2(3) |
| C(1)−W(1)−I(1) | 87.3(4) | I(1)−W(1)−N(51) | 85.6(3) |
| C(1)−W(1)−N(31) | 96.2(5) | N(31)−W(1)−N(41) | 76.1(4) |
| C(1)−W(1)−N(41) | 91.3(5) | N(31)−W(1)−N(51) | 88.5(4) |
| C(1)−W(1)−N(51) | 170.5(5) | N(41)−W(1)−N(51) | 81.8(4) |
| C(6)−W(1)−C(7) | 37.0(5) | W(1)−C(1)−O(1) | 178(1) |
| C(6)−W(1)−I(1) | 97.7(3) | W(1)−C(6)−C(4) | 148(1) |
| C(6)−W(1)−N(31) | 101.0(4) | W(1)−C(7)−C(8) | 141(1) |
| C(6)−W(1)−N(41) | 162.3(4) | C(4)−C(6)−C(7) | 142(1) |
| C(6)−W(1)−N(51) | 115.8(4) | C(6)−C(7)−C(8) | 145(1) |
| C(7)−W(1)−I(1) | 108.9(3) | C(9)−C(8)−C(10) | 112(1) |
| C(7)−W(1)−N(31) | 87.9(4) | C(3)−C(4)−C(5) | 110(1) |
| C(7)−W(1)−N(41) | 156.8(5) | C(4)−C(3)−O(2) | 112(1) |
| C(7)−W(1)−N(51) | 81.1(5) | | |

{PhC≡CH} and in complexes of the type CpMoLL′-(alkyne) where L and L′ differ dramatically in their *π* acidity. [13]

**Extended Hückel Molecular Orbital (EHMO) Calculations.** The alkyne unit in [H$_3$(CO)(I)W-{HC≡CH}]$^{2-}$ is aligned along the W−CO axis in the lowest energy conformation, as expected (Figure 6). In the maximum energy configuration the alkyne is rotated by 90° and aligned along the W−I axis. The calculated barrier to alkyne rotation is 32.2 kcal/mol, higher than the observed barrier to alkyne rotation but compatible with our observation of no alkyne rotation on the NMR time scale at room temperature. Alkyne rotational barriers have been successfully explored with EHMO calculations of simple model compounds in other cases.[23]

To estimate the analogous rotation barrier in the anions generated by deprotonation of Tp′(CO)(I)W{RC≡CCH$_2$R}, EHMO calculations were performed on the model complex [H$_3$(CO)(I)W{HC≡CCH$_2$}]$^{3-}$. The alkyne unit is aligned along the W−CO axis in both energy minima (which differ by about 2.1 kcal/mol) with the CH$_2$ unit proximal to the CO in one and distal in the other (Figure 7). The calculated barrier to deprotonated alkyne rotation is 22.5 kcal/mol, suggesting that rotation is unimportant in the anionic intermediate.

The barrier to enantioface interconversion in the *η*$^2$-allenyl anions was also estimated by EHMO calculations on the model complex [H$_3$(CO)(I)W{HC≡CCH$_2$}]$^{3-}$. The CH$_2$ unit was located in the plane with tungsten

(20) Feng, S. G.; Templeton, J. L. *J. Am. Chem. Soc.* **1989**, *111*, 6477.
(21) Feng, S. G.; Gamble, A. S.; Philipp, C. C.; White, P. S.; Templeton, J. L. *Organometallics* **1991**, *10*, 3504.
(22) Anet, F. A. L.; Bourn, A. J. R. *J. Am. Chem. Soc.* **1967**, *89*, 760.
(23) Templeton, J. L.; Caldarelli, J. L.; Feng, S. G.; Philipp, C. C.; Wells, M. B.; Woodworth, B. E.; White, P. S. *J. Organomet. Chem.* **1994**, *478*, 103.

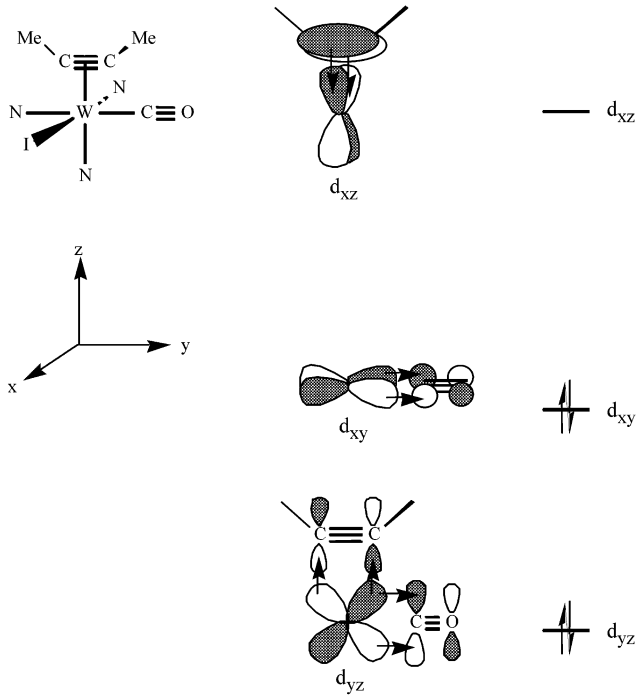


**Figure 4.** Molecular orbital description of Tp′(CO)(I)W-{$CH_3C{\equiv}CCH_3$}.

**Table 4. Selected Bond Distances (Å) and Bond Angles (deg) for $S_WS_C$-(+)-Tp′(CO)W{$CH_3C{\equiv}CCH_3$}(NHCHMePh) ((+)-14(*SS*))**

| | | | |
|---|---|---|---|
| W(1)−C(1) | 1.89(2) | C(1)−O(1) | 1.23(2) |
| W(1)−C(6) | 2.04(1) | C(5)−C(6) | 1.53(2) |
| W(1)−C(7) | 2.10(1) | C(6)−C(7) | 1.27(2) |
| W(1)−N(2) | 1.99(1) | C(7)−C(8) | 1.55(3) |
| W(1)−N(21) | 2.25(1) | N(2)−C(3) | 1.45(2) |
| W(1)−N(31) | 2.29(1) | C(3)−C(4) | 1.51(3) |
| W(1)−N(41) | 2.28(1) | C(3)−C(11) | 1.60(2) |
| C(1)−W(1)−C(6) | 105.8(7) | N(2)−W(1)−N(21) | 83.5(5) |
| C(1)−W(1)−C(7) | 70.4(8) | N(2)−W(1)−N(31) | 91.0(4) |
| C(1)−W(1)−N(2) | 92.0(7) | N(2)−W(1)−N(41) | 165.2(5) |
| C(1)−W(1)−N(21) | 169.1(7) | N(21)−W(1)−N(31) | 79.4(5) |
| C(1)−W(1)−N(31) | 90.8(6) | N(21)−W(1)−N(41) | 85.5(5) |
| C(1)−W(1)−N(41) | 97.0(6) | N(31)−W(1)−N(41) | 77.2(4) |
| C(6)−W(1)−C(7) | 35.7(6) | W(1)−C(1)−O(1) | 173(2) |
| C(6)−W(1)−N(2) | 105.8(5) | W(1)−C(6)−C(5) | 145(1) |
| C(6)−W(1)−N(21) | 85.0(5) | W(1)−C(7)−C(8) | 147(1) |
| C(6)−W(1)−N(31) | 155.6(5) | C(5)−C(6)−C(7) | 140(1) |
| C(6)−W(1)−N(41) | 83.0(5) | C(6)−C(7)−C(8) | 144(2) |
| C(7)−W(1)−N(2) | 102.6(5) | W(1)−N(2)−C(3) | 133(1) |
| C(7)−W(1)−N(21) | 120.3(6) | N(2)−C(3)−C(4) | 113(2) |
| C(7)−W(1)−N(31) | 156.9(6) | N(2)−C(3)−C(11) | 112(1) |
| C(7)−W(1)−N(41) | 91.5(5) | | |

and the rest of the $[HC{\equiv}CCH_2]^-$ ligand in the lowest energy conformation (Figure 8). The barrier to rotation of the $CH_2$ unit was calculated to be 27.5 kcal/mol, perhaps less than one would anticipate. Regardless, this enantioface interconversion barrier is adequate to maintain a static structure during electrophile addition.

**Isolation of Free Alkynes.** The alkyne ligand is bound tightly to the Tp′(CO)(I)W fragment, but it can be dislodged by photolysis. THF solutions of Tp′(CO)-(I)W{alkyne} were photolyzed in air to produce free alkyne in yields of 82−97%, as determined by gas chromatography using nonane as an internal standard. The fate of the metal fragment is unknown.

Isolation of the free alkyne was accomplished by alumina filtration of the hexane or pentane extract of the solid residue obtained after photolysis (Scheme 3). This method was used to isolate $PhC{\equiv}CCH_3$ and $CH_3C{\equiv}CCHMeCH_2Ph$. Failure to isolate the alcohol-functionalized alkyne from the Tp′(CO)(I)W{$CH_3C{\equiv}C$-$CH_2CH(OH)Ph$} complex suggests that a metal intermediate may react with the hydroxyl functional group during photolysis.

**Regioselectivity of Elaboration.** Excellent regiocontrol is exhibited in the elaboration of Tp′(CO)(I)W-{$CH_3C{\equiv}CCH_3$}. Single isomers were obtained by the

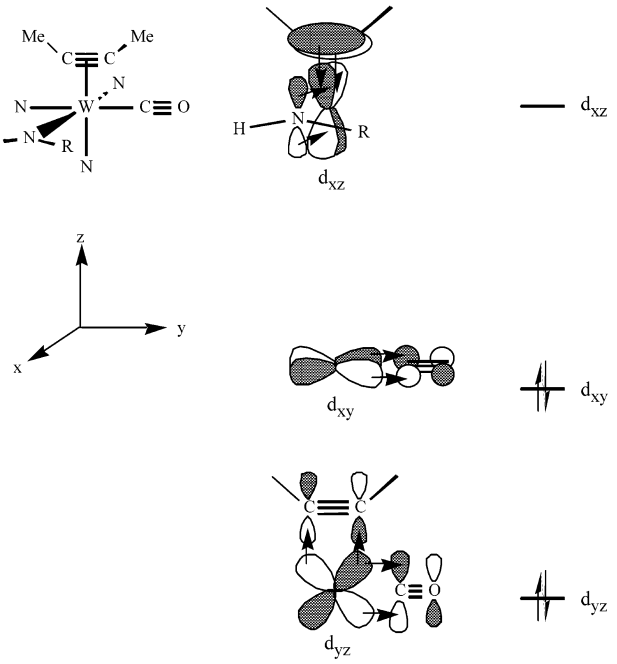


**Figure 5.** Molecular orbital description of Tp′(CO)W-{$CH_3C{\equiv}CCH_3$}(NHR).

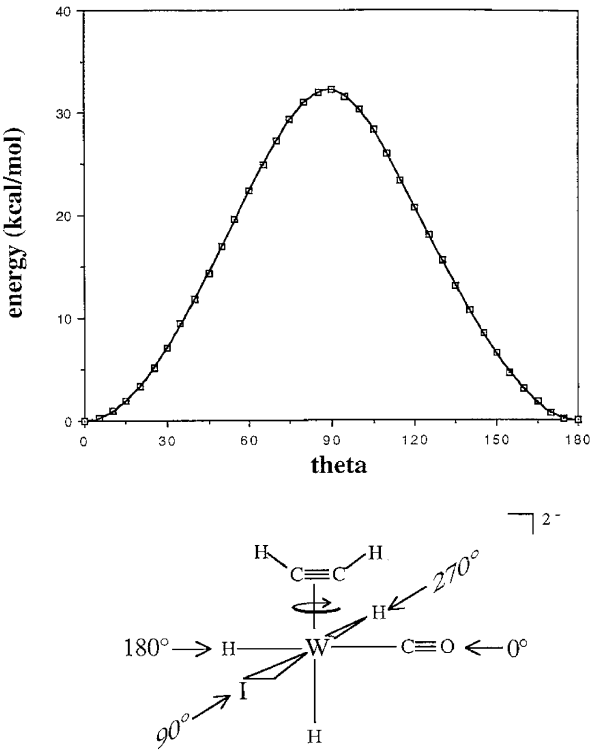


**Figure 6.** EHMO calculation of alkyne rotation in $[H_3(CO)(I)W\{HC{\equiv}CH\}]^{2-}$.

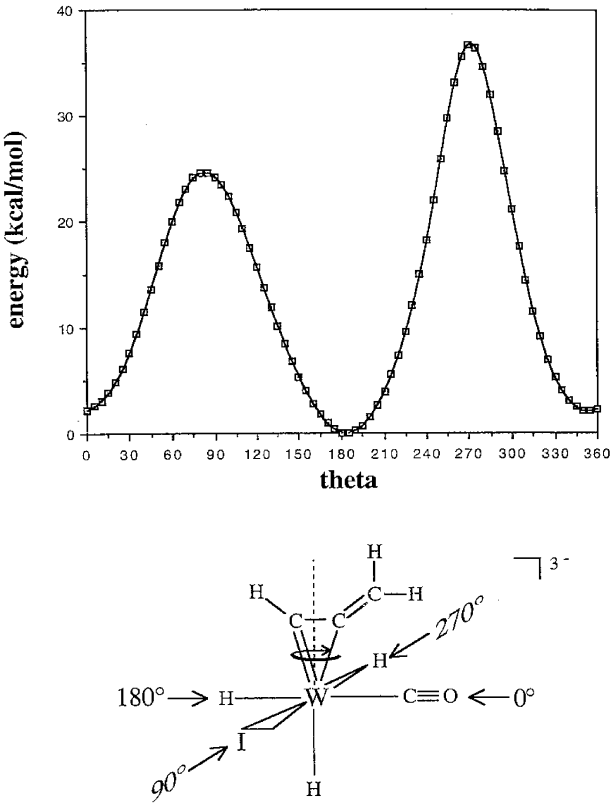


**Figure 7.** EHMO calculation of deprotonated alkyne rotation in $[H_3(CO)(I)W\{HC{\equiv}CCH_2\}]^{3-}$.

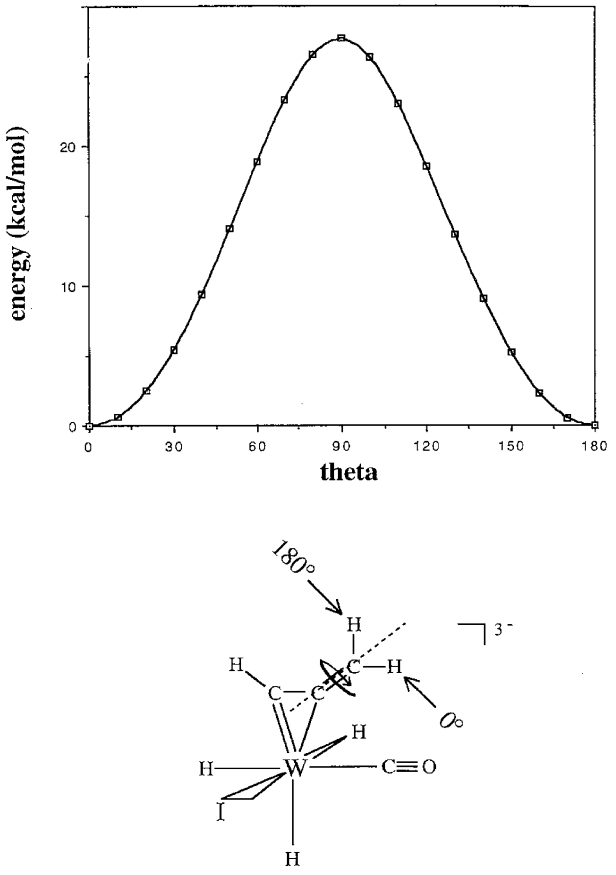


**Figure 8.** EHMO calculation of enantioface interconversion in $[H_3(CO)(I)W\{HC{\equiv}CCH_2\}]^{3-}$.

addition of various electrophiles to the $\eta^2$-allenyl anion formed by deprotonating **1**. Electrophiles add exclusively

**Scheme 3**

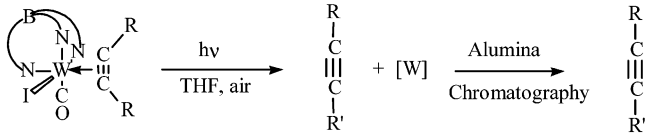


**Scheme 4**

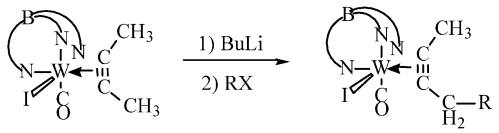


RX = MeI (**2**), $PhCH_2Br$ (**3**), $I(CH_2)_3I$ (**4**), Ph-C(=O)-H + $H^+$ (**5**)

**Scheme 5**

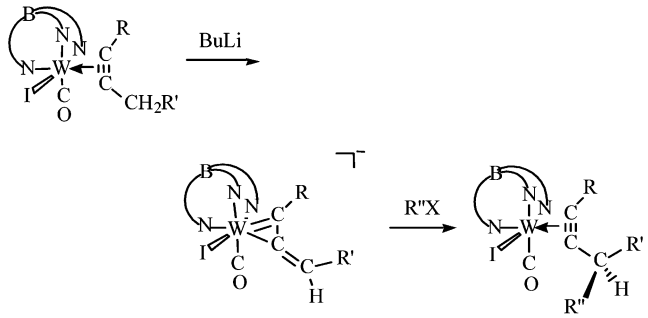


R, R', R"X =

Me, Me, EtI (**6**);

Me, Me, $I(CH_2)_4I$ (**7**);

Me, Me, $PhCH_2Br$ (**8a**);

Me, -$CH_2Ph$, MeI (**8b**);

Et, Me,$PhCH_2Br$ (**10**).

to the syn propargyl carbon of deprotonated **1** (Scheme 4). The singlet at 3.49 ppm in the $^1H$ NMR spectrum has been assigned to the syn methyl group of the alkyne in **1** (Chart 2) on the basis of comparison with the chemical shift of the syn methyl group of Tp′(CO)(I)W{PhC≡$CCH_3$} at 3.54 ppm. The anti methyl of **1** is sandwiched between two aromatic pyrazole rings, and its chemical shift of 2.62 ppm, on the basis of the COSY NMR spectrum, is almost 1 ppm upfield from the syn methyl in **1**. No syn methyl singlet appears in $^1H$ NMR spectra of the crude reaction mixture resulting from the elaboration of **1,** thus indicating that reaction occurred exclusively at the syn methyl.

With only one exception, electrophiles added to the $\eta^2$-allenyl anion formed from $CH_3C{\equiv}CCH_2R$ to produce a tertiary syn propargyl carbon in preference to a secondary anti propargyl carbon (Scheme 5). The exception to exclusive syn addition is the 9:1 mixture of Tp′(CO)(I)W{$CH_3C{\equiv}CCHMe_2$} (syn addition) to Tp′(CO)(I)W{$CH_3CH_2C{\equiv}CCH_2CH_3$} (anti addition) obtained from the addition of methyl iodide to deprotonated **2**. All other double elaborations resulted in products with both electrophiles added to the syn propargyl carbon. The presence of only the syn isomer was indicated by the $^1H$ NMR spectra of the products obtained in forming **8a** and **8b** taken before chromatography or recrystallization.

Clearly the syn propargyl carbon site is more susceptible to deprotonation than the anti position; therefore,

**Scheme 6**

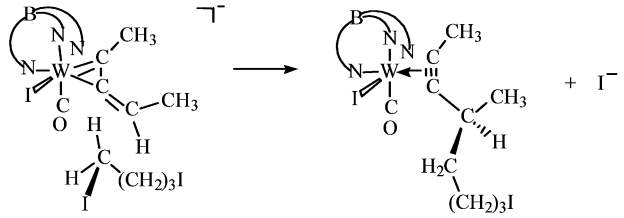

**7**

**Scheme 7**

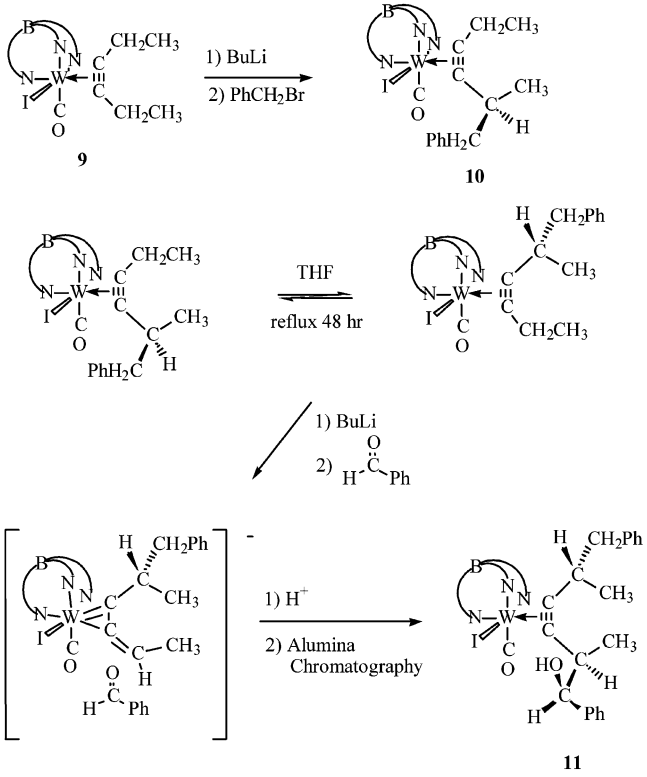

**9** **10** **11**

a single $\eta^2$-allenyl isomer is formed preferentially. Inspection of the X-ray structures of **7** and **11** suggests that the pendant methyl groups of Tp′ effectively block access to the anti site and lead to the observed regioselectivity.

**Stereoselectivity of Electrophilic Addition.** Electrophilic addition of alkyl halides and benzaldehyde to the $\eta^2$-allenyl anion formed by deprotonating Tp′(CO)(I)W{RC≡CCH$_2$R′} (R = Me, Et, −CHMe(CH$_2$Ph); CH$_2$R′ = Me, Et, −CH$_2$CH$_2$Ph) is stereoselective (Scheme 5). Benzylation of **2** yields a single diastereomer (**8a**) while methylation of **3** yields the opposite diastereomer (**8b**).

The origin of this stereoselectivity is suggested by the crystal structure of **7** (Figure 1). The position of the −(CH$_2$)$_4$I unit in **7** is compatible with the electrophilic addition of I(CH$_2$)$_4$I parallel to the I−W axis to a single face of the $\eta^2$-allenyl anion [Tp′(CO)(I)W{CH$_3$C≡CCH-CH$_3$}]$^-$ if one assumes that the methyl group is trans to the bulky metal center (Scheme 6). We have no direct data relevant to location of the methyl group in the $\eta^2$-allenyl intermediate.

Inspection of the stereochemistry of the −CH(Me)-(CH$_2$Ph) unit (constructed at the syn site and allowed to rotate, Scheme 7) in the X-ray structure of **11** (Figure 2) leads to the same conclusions about the stereochemistry of benzylation of the syn propargyl carbon of Tp′-(CO)(I)W{CH$_3$CH$_2$C≡CCH$_2$CH$_3$} (Scheme 7). Likewise, the stereochemistry of aldehyde addition to the syn propargyl carbon of Tp′(CO)(I)W{(PhCH$_2$)(Me)CHC≡C-CH$_2$CH$_3$} to give the −CH(Me)(CH(OH)Ph) unit is controlled by the same factors. Furthermore, the chirality of the alcohol carbon is also controlled by the metal center. A possible explanation for the stereocontrol of this alcohol carbon is that benzaldehyde approaches a single face of the $\eta^2$-allenyl anion parallel to the I−W axis with the phenyl group directed away from the metal center (Scheme 7).

**Scheme 8**

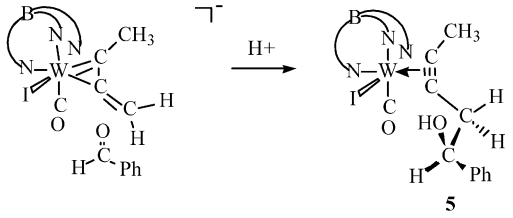

**5**

A single diastereomer of Tp′(CO)(I)W{CH$_3$C≡CCH$_2$-CH(OH)Ph} (**5**) is also formed by benzaldehyde addition to the anion [Tp′(CO)(I)W{CH$_3$C≡CCH$_2$}]$^-$, presumably because aldehyde addition occurs in the same manner as for **11** (Scheme 8).

The stereoselectivity of the electrophilic additions reported here presumably mimics the stereoselectivity of the $\eta^2$-allenyl anion formed by deprotonating Tp′(CO)-(I)W{PhC≡CCH$_2$R}.[10] The X-ray structures of **11** and Tp′(CO)(I)W{PhC≡CCHMeCH(OH)Ph} reveal a common stereochemistry for the −CHMeCH(OH)Ph fragment. The fact that the stereochemistry is the same for both −CHMeCH(OH)Ph fragments suggests that the chiral Tp′(CO)IW fragment controls the stereochemistry of electrophilic addition in both the phenyl−alkyne and the alkyl−alkyne complexes.

**Optical Resolution of Tp′(CO)(I)W{CH$_3$C≡CCH$_3$}.** Resolution of Tp′(CO)(I)W{CH$_3$C≡CCH$_3$} (Scheme 9) follows the literature procedure for the resolution of Tp′-(CO)(I)W{PhC≡CCH$_3$}.[12] Racemic Tp′(CO)(I)W{CH$_3$C≡CCH$_3$} **(1)** was converted to the neutral triflate complex Tp′(CO)(OTf)W{CH$_3$C≡CCH$_3$} **(13)** by the addition of silver triflate. This racemic [W]−OTf complex can be refluxed in THF with 2 equiv of the optically pure (*S*)-(−)-α-methylbenzylamine to produce a pair of amido diastereomers, **14(*SS*)** and **14(*RS*)**. (This nomenclature refers to the tungsten configuration first and ligand configuration second.) Alumina chromatography purifies this mixture but does not separate the diastereomers. Several crystallizations with CH$_2$Cl$_2$/pentane afford the less soluble **14(*SS*)** (the configuration was assigned on the basis of its X-ray crystal structure; see above). The supernatant contained a 4:1 (**14(*RS*)**:**14(*SS*)**) ratio of diastereomers. This enriched mixture was protonated with HBF$_4$ to yield a 4:1 (**15(*RS*)**:**15(*SS*)**) mixture of cationic amine diastereomers. Several recrystallizations of the mixture of amine complexes afforded pure *RS* diastereomer. Pure RS amido complex (**14(*RS*)**) was then obtained by deprotonation of the RS amine complex with butyllithium.

Each amido isomer was independently characterized by IR, optical rotation, elemental analysis, $^1$H NMR, and $^{13}$C NMR. The carbonyl stretching bands for the two

**Scheme 9**

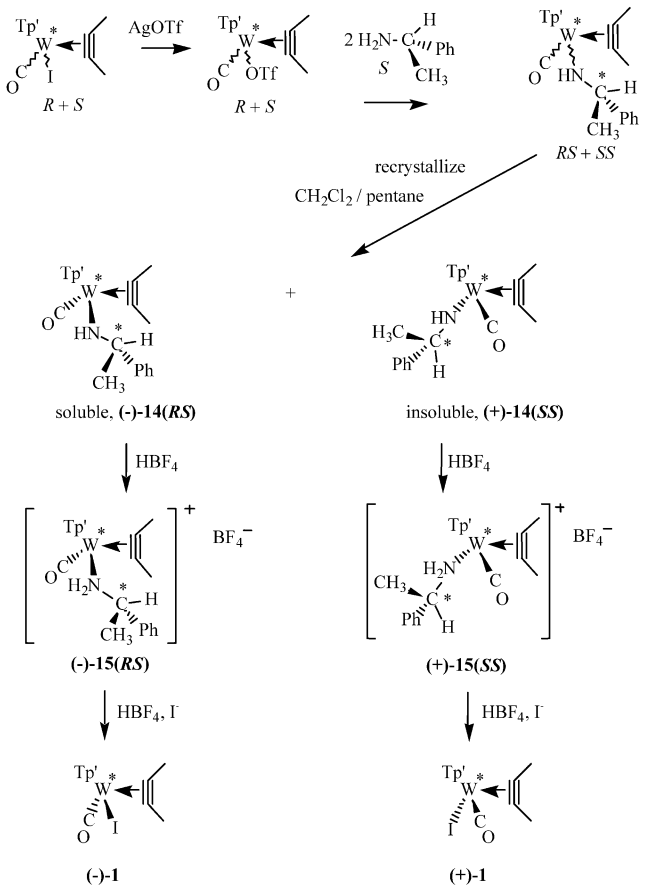


**Table 5. Optical Rotations (deg) for Resolved Compounds**[a]

| compd | $[\alpha]^{25}_{589}$ |
|---|---|
| ($S_W$,$S_C$)-(+)-Tp′(CO)W{$CH_3C{\equiv}CCH_3$}(NHR) **((+)−14(*RS*))** | +110 |
| ($R_W$,$S_C$)-(−)-Tp′(CO)W{$CH_3C{\equiv}CCH_3$}(NHR) **((−)-14(*RS*))** | −340 |
| ($S_W$,$S_C$)-(+)-[Tp′(CO)W{$CH_3C{\equiv}CCH_3$}($NH_2R$)][$BF_4$] **((+)−15(*SS*))** | +520 |
| ($R_W$,$S_C$)-(−)-[Tp′(CO)W{$CH_3C{\equiv}CCH_3$}($NH_2R$)][$BF_4$] **((−)-15(*RS*))** | −280 |
| (+)-Tp′(CO)(I)W{$CH_3C{\equiv}CCH_3$} **((+)-1)** | +740 |
| (−)-Tp′(CO)(I)W{$CH_3C{\equiv}CCH_3$} **((−)-1)** | −730 |
| (+)-Tp′(CO)(I)W{$CH_3C{\equiv}CCH_2CH_3$} **((+)-2)** | +730 |
| (−)-Tp′(CO)(I)W{$CH_3C{\equiv}CCH_2CH_3$} **((−)-2)** | −740 |
| (+)-Tp′(CO)(I)W{$CH_3C{\equiv}CCHMeCH_2Ph$} **((+)-8a)** | +850 |
| (−)-Tp′(CO)(I)W{$CH_3C{\equiv}CCHMeCH_2Ph$} **((−)-8a)** | −850 |
| (−)-$CH_3C{\equiv}CCHMeCH_2Ph$ | −56 |
| (+)-$CH_3C{\equiv}CCHMeCH_2Ph$ | +52 |

[a] $NH_2R$ = (*S*)-(−)-α-methylbenzylamine.

isomers were not significantly different (**14(*SS*)**, $\nu_{CO}$ 1839 $cm^{-1}$; **14(*RS*)**, $\nu_{CO}$ = 1838 $cm^{-1}$), but $^1H$ NMR and $^{13}C$ NMR spectra differ significantly. The methyl doublet for the coordinated amide in **14(*SS*)** appears at 1.22 ppm, while the corresponding methyl doublet in **14(*RS*)** appears at 0.87 ppm. The $^{13}C$ NMR signal for the chiral carbon of the amide ligand appears at 71.5 and 72.5 ppm for the *SS* and *RS* isomers, respectively. The optical rotations were found to be $[\alpha]^{25}_{589}$ = +110° for **14(*SS*)** and $[\alpha]^{25}_{589}$ = −340° for **14(*RS*)**. Optical rotations for the resolved complexes are presented in Table 5. As one might expect, the two optical rotations are opposite in sign but the magnitudes are unequal for these diastereomers, which are both *S* at carbon. The X-ray structure of **14(*SS*)**, described above, was used to assign the *S* configuration at tungsten using the *S* configuration of the amide ligand as reference.

Protonation of the amido complex to form the cationic amine complex is easily accomplished by the addition of $HBF_4$. The methyl doublet for the coordinated amine in **15(*SS*)** appears at 1.70 ppm, while the corresponding methyl doublet in **15(*RS*)** appears at 1.05 ppm. The $^{13}C$ NMR signal for the chiral carbon of the amine ligand appears at 62.5 and 63.5 ppm for the *SS* and *RS* isomers, respectively. No trace of the other diastereomer was observed in the $^1H$ NMR spectra of the amine complexes, which were subsequently converted to optically pure iodide complexes. Substitution of the same resolving amine in the closely related Tp′(CO)(NHR)W{$PhC{\equiv}CCH_3$} (R = (*S*)-(−)-α-methylbenzylamine) complex has been achieved without racemization of the metal center.[12]

Protonation of each of the amine diastereomers with $HBF_4$ in the presence of iodide affords each enantiomer of Tp′(CO)(I)W{$CH_3C{\equiv}CCH_3$} (Scheme 9). The optical rotation of the enantiomer generated from **(+)-15(*SS*)** was found to be $[\alpha]^{25}_{589}$ = +740°, while an optical rotation of $[\alpha]^{25}_{589}$ = −730° was found for the enantiomer generated from **(−)-15(*RS*)**.

**Synthesis of Racemic and Optically Pure $CH_3C{\equiv}CCHMeCH_2Ph$.** Isolation of $CH_3C{\equiv}CCHMeCH_2Ph$ from racemic **8a** was accomplished using a photolysis procedure. Methylation of optically pure **(+)-1** or **(−)-1** forms **(+)-2** or **(−)-2** (Scheme 10). Photolysis allowed the isolation of (−)-$CH_3C{\equiv}CCHMeCH_2Ph$ and (+)-$CH_3C{\equiv}CCHMeCH_2Ph$ from **(+)-8a** and **(−)-8a**, respectively (Scheme 11).

The optical purity of (−)-$CH_3C{\equiv}CCHMeCH_2Ph$ was assayed by $^1H$ NMR using chiral shift reagent techniques. A scalemic mixture which contained 90% (−)-$CH_3C{\equiv}CCHMeCH_2Ph$ and 10% (+)-$CH_3C{\equiv}CCHMeCH_2Ph$ was prepared from (−)-$CH_3C{\equiv}CCHMeCH_2Ph$ isolated from **(+)-8a** and racemic $CH_3C{\equiv}CCHMeCH_2Ph$ isolated from racemic **8a**. The presence of the minor isomer was clearly visible in the $^1H$ NMR spectrum. Since only one enantiomer could be detected in the $^1H$ NMR spectra of (−)-$CH_3C{\equiv}CCHMeCH_2Ph$ in the presence of various concentrations of the chiral shift reagents, an ee of greater than 80% is inferred.

The optical rotation of (−)-$CH_3C{\equiv}CCHMeCH_2Ph$ was found to be −56 ± 10°. The optical rotation of (+)-$CH_3C{\equiv}CCHMeCH_2Ph$ yielded a value of +52 ±10°. The small amount of alkyne available limited the accuracy of these measurements, but the fact that the two values are similar in magnitude and opposite in sign is indicative of configurational stability during all of the reactions including the photolysis. The data are consistent with high optical purity for each enantiomer of $CH_3C{\equiv}CCHMeCH_2Ph$.

## Summary

Elaborations of the propargyl carbon in complexes of the type Tp′(CO)(I)W{RC≡CR′} were shown to occur selectively at the syn propargyl carbon. The steric bulk of the Tp′ ligand directs the chemistry to the syn propargyl carbon, while the large alkyne rotational

**Scheme 10. Diastereoselective Alkyne Elaboration Reactions of Resolved 1**

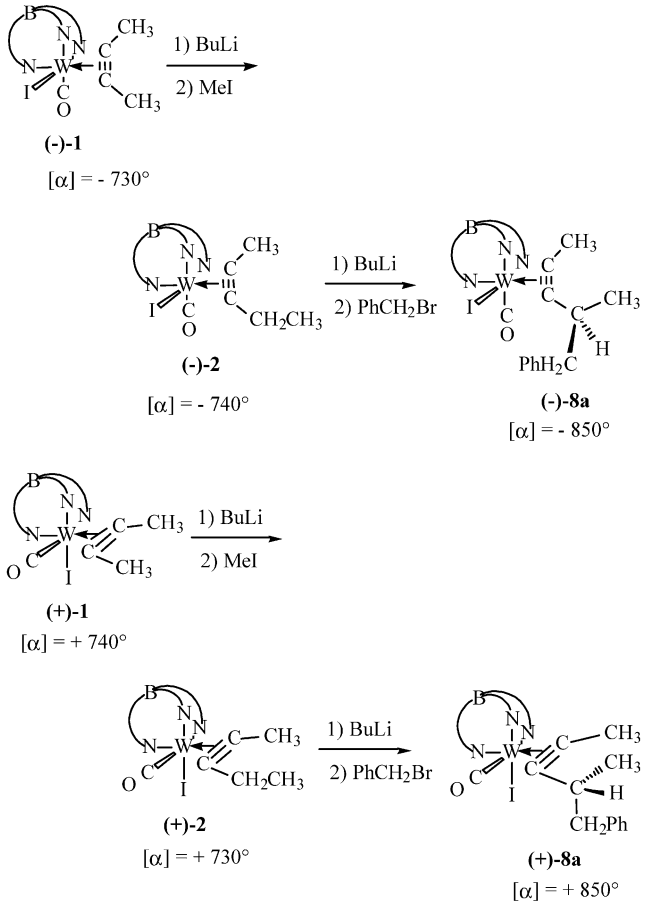


**Scheme 11. Isolation of Optically Pure Alkynes**

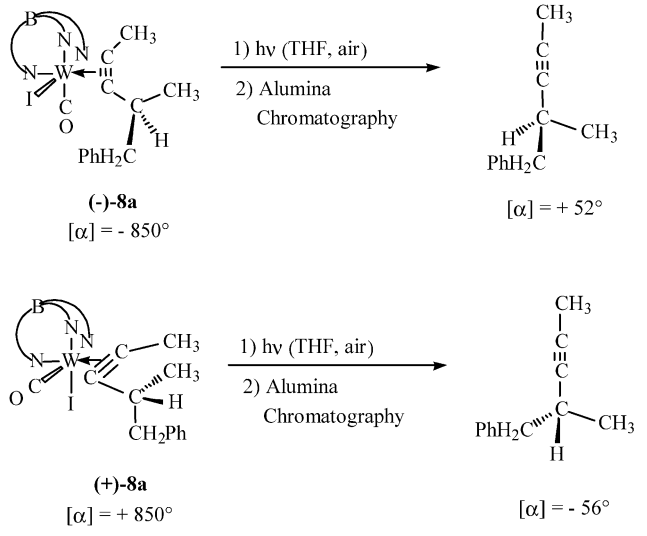


barrier prevents scrambling of the two alkyne ends. The addition reactions were also shown to be stereoselective. A photolytic procedure for decomplexation and isolation of the alkyne from the chiral metal center was developed. Optical resolution of the Tp′(CO)(I)W{$CH_3C{\equiv}CCH_3$} complex via separation of a pair of amido diastereomers was achieved. Regioselective and stereoselective elaboration of an optically pure complex led to the isolation of free alkyne with an ee of >80%.

## Experimental Section

**Tp′(CO)(I)W{$CH_3C{\equiv}CCH_2CH_3$} (2).** To a green solution of Tp′(CO)(I)W{$CH_3C{\equiv}CCH_3$}[21] (2.00 g, 2.89 mmol) in THF, cooled to −78 °C, was added butyllithium (2.03 mL, 5.07 mmol). To the resulting red-brown solution was added iodomethane (1.80 mL, 28.9 mmol) through a layer of alumina. The color of the solution immediately changed to green. The solvent was removed, leaving a green oil. The oil was chromatographed on alumina, and a green band was eluted with methylene chloride. The solvent was removed, leaving the green solid product (yield 1.91 g, 2.71 mmol, 94%). IR (KBr): $\nu_{CO}$ 1904 cm$^{-1}$. $^1$H NMR ($\delta$, $CD_2Cl_2$): 6.12, 5.85, 5.71 (3 s, Tp′ C−*H*); 3.77 (dq, 1 H, $^2J_{HH}$ = 14.8 Hz, $^3J_{HH}$ = 7.4 Hz, −C*H*HCH$_3$); 3.40 (dq, 1 H, $^2J_{HH}$ = 14.8 Hz, $^3J_{HH}$ = 7.4 Hz, −CH*H*CH$_3$); 2.83, 2.67, 2.56, 2.45, 2.34, 1.45 (6 s, 3:3:3:3:6:3 H, Tp′ C$H_3$ and C$H_3$C≡C); 1.54 (t, 3H, $^3J_{HH}$ = 7.4 Hz, −CHHC$H_3$). $^{13}$C NMR ($\delta$, $CD_2Cl_2$): 233.5 (s, *C*O); 211.4, 204.8 (2 s, *C*≡*C*); 155.4, 154.2, 150.0, 145.6, 145.4, 144.4 (6 s, Tp′ *C*−CH$_3$); 108.3, 108.1, 107.0 (3 s, Tp′ *C*−H); 31.5, 20.2, 19.2, 18.3, 16.3, 13.3, 12.9, 12.8, 12.7, (9 s, Tp′ *C*H$_3$ and *C*H$_3$C≡C*C*H$_2$*C*H$_3$). Anal. Calcd for $C_{21}H_{30}N_6WBOI$: C, 35.82; H, 4.29; N, 11.94. Found: C, 35.90; H, 4.24; N, 11.88.

**Tp′(CO)(I)W{$CH_3C{\equiv}CCH_2CH_2Ph$} (3).** To a green solution of Tp′(CO)(I)W{$CH_3C{\equiv}CCH_3$} (1.440 g, 2.08 mmol) in THF, cooled to −78 °C, was added butyllithium (1.50 mL, 3.75 mmol). To the resulting red-brown solution was added benzyl bromide (2.49 mL, 20.8 mmol). The color of the solution changed to blue-green over 30 min. The solvent was removed, leaving a blue-green oil. The oil was chromatographed on alumina, and a blue-green band was eluted with methylene chloride. The solvent was removed, leaving a blue solid. Blue crystals were obtained by layering hexane on a methylene chloride solution of the blue solid (yield 1.163 g, 1.49 mmol, 72%). IR (KBr): $\nu_{CO}$ 1898 cm$^{-1}$. $^1$H NMR ($\delta$, $CD_2Cl_2$): 7.3−7.0 (m, 5 H, Ph); 6.13, 5.89, 5.72 (3 s, Tp′ C−*H*); 4.14, 3.94, 3.34, 3.06 (4 m, 1 H each, −C*H*$_2$C*H*$_2$Ph); 2.90, 2.59, 2.44, 2.37, 2.30, 2.29, 1.46 (7 s, 3 H each, Tp′ C$H_3$ and C$H_3$C≡C). $^{13}$C NMR ($\delta$, $CD_2Cl_2$): 234.2 (s, *C*O); 212.9, 203.0 (2 s, *C*≡*C*); 155.4, 154.2, 149.8, 145.6, 145.5, 144.3 (6 s, Tp′ *C*−CH$_3$); 141.6, 129.0, 128.7, 126.4 (4 s, Ph); 108.3, 108.2, 107.0 (3 s, Tp ′*C*−H); 38.7, 33.5 (2 s, −C*C*H$_2$*C*H$_2$Ph)); 19.8, 19.0, 18.4, 16.3, 12.9, 12.8, 12.7 (7 s, Tp′ *C*H$_3$ and *C*H$_3$C≡C). Anal. Calcd for $C_{27}H_{34}N_6WBOI$: C, 41.57; H, 4.39; N, 10.77. Found: C, 41.62; H, 4.38; N, 10.76.

**Tp′(CO)(I)W{$CH_3C{\equiv}C(CH_2)_4I$} (4).** To a green solution of Tp′(CO)(I)W{$CH_3C{\equiv}CCH_3$} (5.00 g, 7.23 mmol) in THF, cooled to −78 °C, was added butyllithium (4.92 mL, 12.3 mmol). To the resulting red-brown solution was added 1,3-diiodopropane (4.16 mL, 36.2 mmol). The color of the solution changed to green over 5 min. The solvent was removed, leaving a green oil. The oil was chromatographed on alumina, and a green band was eluted with methylene chloride. The solvent was removed, leaving a green oil. Green crystals were obtained by layering hexane on a methylene chloride solution of the green oil (yield 5.30 g, 6.18 mmol, 85%). IR (KBr): $\nu_{CO}$ 1898 cm$^{-1}$. $^1$H NMR ($C_6D_5Br$): $\delta$ 6.14, 5.64, 5.60 (3 s, Tp′ C−*H*); 3.87, 3.70 (2 m, 1 H each, −CC*H*$_2$(CH$_2$)$_3$I); 3.16 (s, 3 H, C*H*$_3$C≡C); 3.15 (t, 2H, $^3J_{HH}$ = 6.8 Hz, −C*H*$_2$I); 2.84, 2.65, 2.53, 2.38, 2.25, 1.58 (6 s, 3 H each, Tp′ C*H*$_3$); 2.10, 1.75 (2 m, 2 H each, −CH$_2$C*H*$_2$C*H*$_2$CH$_2$I). $^{13}$C NMR ($\delta$, $CD_2Cl_2$): 234.0 (s, *C*O); 211.9, 203.0 (2 s, *C*≡*C*); 155.5, 154.2, 150.0, 145.8, 145.6, 144.5 (6 s, Tp′ *C*−CH$_3$); 108.4, 108.2, 107.1 (3 s, Tp′ *C*−H); 36.1, 33.7, 29.3, 20.3, 19.3, 18.4, 16.4, 13.0, 12.8, 12.7 (10 s, Tp′ *C*H$_3$ and *C*H$_3$C≡C(CH$_2$)$_3$CH$_2$I)); 7.1 (s, −*C*H$_2$I). Anal. Calcd for $C_{25}H_{37}N_6WBOI_2$: C, 32.20 H, 3.88; N, 9.79. Found: C, 32.38; H, 4.00; N, 9.85.

**Tp′(CO)(I)W{$CH_3C{\equiv}CCH_2CH(OH)Ph$} (5).** To a green solution of Tp′(CO)(I)W{$CH_3C{\equiv}CCH_3$} (0.100 g, 0.144 mmol) in THF, cooled to −78 °C, was added butyllithium (0.086 mL, 0.216 mmol). To the resulting red-brown solution was added benzaldehyde (0.087 mL, 0.72 mmol). The color of the solution

changed to green immediately. The reaction was quenched by the addition of HCl (0.22 mL of 1.0 M HCl in diethyl ether, 0.216 mmol). The solvent was removed leaving a green oil. The oil was chromatographed on alumina, and a green band was eluted with methanol. The solvent was removed leaving a green oil. The oil was taken up in methylene chloride and layered with hexanes to obtain green crystals (yield 0.079 g, 0.099 mmol, 69%). IR (KBr): $\nu_{CO}$ 1900 cm$^{-1}$. $^1$H NMR ($\delta$, $CD_2Cl_2$): 7.5−7.2 (m, 5 H, Ph); 6.11, 5.87, 5.68 (3 s, Tp′ C−*H*); 5.07 (ddd, 1 H, $^3J_{HH}$ = 7 Hz, $^3J_{HH}$ = 5.9 Hz, $^3J_{HH}$ = 3.1 Hz, −CHHC*H*(OH)Ph); 4.29 (dd, 1 H, $^2J_{HH}$ = 14 Hz, $^3J_{HH}$ = 5.9 Hz, −C*H*HCH(OH)Ph); 4.18 (dd, 1 H, $^2J_{HH}$ = 14 Hz, $^3J_{HH}$ = 7 Hz, −CH*H*CH(OH)Ph); 2.87, 2.55, 2.41, 2.34, 2.33, 2.27, 1.40 (7 s, 3 H each, Tp′ C*H*$_3$ and C*H*$_3$C≡C); 2.44 (d, 1 H, $^3J_{HH}$ = 3.1 Hz, −CHHCH(O*H*)Ph). $^{13}$C NMR ($\delta$, $CD_2Cl_2$): 233.7 (s, *C*O); 215.1, 201.2 (2 s, *C*≡*C*); 155.6, 154.8, 149.8, 145.8, 145.6, 144.4 (6 s, Tp′ *C*−CH$_3$); 144.1, 128.8, 128.2, 126.5, (4 s, Ph); 108.4, 108.3, 107.1 (3 s, Tp′ *C*−H); 72.9 (s, −*C*H(OH)Ph); 46.7 (s, −*C*HHCH(OH)Ph); 19.9, 19.2, 18.4, 16.4, 13.0, 12.8, 12.7 (7 s, Tp′ *C*H$_3$ and *C*H$_3$C≡C). Anal. Calcd for $C_{27}H_{34}N_6WBO_2I$: C, 40.37; H, 4.30; N, 10.56. Found: C, 40.75; H, 4.23; N, 10.58.

**Tp′(CO)(I)W{CH$_3$C≡CCH(Me)(CH$_2$CH$_3$)} (6)**. To a green solution of Tp′(CO)(I)W{CH$_3$C≡CCH$_2$CH$_3$} (1.171 g, 1.66 mmol) in THF, cooled to −78 °C, was added butyllithium (1.00 mL, 2.50 mmol). To the resulting red-brown solution was added iodoethane (0.66 mL, 8.30 mmol). The color of the solution changed to green. The solvent was removed, leaving a green oil, which was then chromatographed on alumina, and a green band was eluted with methylene chloride. The solvent was removed, leaving a green powder (yield 0.951 g, 1.30 mmol, 78%). IR (KBr): $\nu_{CO}$ 1900 cm$^{-1}$. $^1$H NMR ($\delta$, $CD_2Cl_2$): 6.16, 5.88, 5.76 (3 s, Tp′ C−*H*); 3.91 (m, 1 H, −C*H*(CH$_3$)(CH$_2$CH$_3$)); 2.87, 2.70, 2.61, 2.47, 2.38, 2.35, 1.58 (7 s, 3 H each, Tp′ C*H*$_3$ and C*H*$_3$C≡C); 2.05, 1.68 (2 m, 1 H each, −CH(CH$_3$)(C*H*HCH$_3$)); 1.72 (d, 3 H, $^3J_{HH}$ = 6.8 Hz, −CH(CH$_3$)(CHHCH$_3$)); 0.88 (t, 3 H, $^3J_{HH}$ = 7.4 Hz, −CH(CH$_3$)(CHHC*H*$_3$)). $^{13}$C NMR ($\delta$, $CD_2Cl_2$): 233.9 (s, *C*O); 211.5, 206.0 (2 s, *C*≡*C*); 155.4, 154.0, 150.0, 145.8, 145.4, 144.3 (6 s, Tp′ *C*−CH$_3$); 108.4, 108.1, 107.1 (3 s, Tp′ *C*−H); 43.0 (s, −*C*H(CH$_3$)(CH$_2$CH$_3$); 26.8, 20.5, 19.3, 18.9, 18.5, 16.4, 13.0, 12.9, 12.8, 10.1 (10 s, Tp′ *C*H$_3$ and *C*H$_3$C≡CCH(*C*H$_3$)(*C*H$_2$*C*H$_3$)). Anal. Calcd for $C_{23}H_{34}N_6WBOI$: C, 37.73; H, 4.68; N, 11.48. Found: C, 37.84; H, 4.70; N, 11.45.

**Tp′(CO)(I)W{CH$_3$C≡CCHMe(CH$_2$)$_4$I} (7)**. To a green solution of Tp′(CO)(I)W{CH$_3$C≡CCH$_2$CH$_3$} (1.009 g, 1.43 mmol) in THF, cooled to −78 °C, was added butyllithium (1.00 mL, 2.50 mmol). To the resulting red-brown solution was added 1,4-diiodobutane (1.89 mL, 14.3 mmol). The color of the solution changed to green over 30 min. The solvent was removed, leaving a green oil. The oil was chromatographed on alumina, and a green band was eluted with methylene chloride. The solvent was removed, leaving the green solid product (yield 1.008 g, 1.14 mmol, 80%). IR (KBr): $\nu_{CO}$ 1894 cm$^{-1}$. $^1$H NMR ($\delta$, $CD_2Cl_2$): 6.13, 5.85, 5.73 (3 s, Tp′ C−*H*); 3.93 (m, 1 H, −C*H*(CH$_3$)[(CH$_2$)$_4$I]); 3.21 (m, 2H, −C*H*$_2$I); 2.85, 2.68, 2.58, 2.44, 2.35, 2.32, 1.54 (7 s, 3 H each, Tp′ C*H*$_3$ and C*H*$_3$C≡C); 1.98, 1.88, 1.70, 1.51, 1.06 (5 m, 1:2:1:1:1 H, −CH(CH$_3$)[(C*H*$_2$)$_3$CH$_2$I]); 1.71 (d, 3 H, $^3J_{HH}$ = 6.7 Hz, −CH(C*H*$_3$)[(CH$_2$)$_4$I]). $^{13}$C NMR ($\delta$, $CD_2Cl_2$): 233.9 (s, *C*O); 211.5, 205.6 (2 s, *C*≡*C*); 155.4, 154.1, 150.0, 145.8, 145.4, 144.4 (6 s, Tp′ *C*−CH$_3$); 108.4, 108.1, 107.0 (3 s, Tp′ *C*−H); 41.6 (s, −*C*H(CH$_3$)[(CH$_2$)$_3$CH$_2$I]); 33.6, 32.5, 27.2, 20.5, 19.4, 19.3, 18.5, 16.3, 12.9, 12.8, 12.7 (11 s, Tp′ *C*H$_3$ and *C*H$_3$C≡CCH(*C*H$_3$)[(*C*H$_2$)$_3$CH$_2$I]); 8.1 (s, −*C*H$_2$I). Anal. Calcd for $C_{25}H_{37}N_6WBOI_2$: C, 33.89; H, 4.21; N, 9.48. Found: C, 33.89; H, 4.16; N, 9.49.

**Tp′(CO)(I)W{CH$_3$C≡CCHMeCH$_2$Ph} (8a)**. To a green solution of Tp′(CO)(I)W{CH$_3$C≡CCH$_2$CH$_3$} (0.735 g, 1.04 mmol) in THF, cooled to −78 °C, was added butyllithium (0.75 mL, 1.87 mmol). To the resulting red-brown solution was added benzyl bromide (1.78 g, 10.4 mmol). The color of the solution changed to blue-green over 30 min. The solvent was removed, leaving a blue-green oil. The oil was chromatographed on alumina, and a blue-green band was eluted with methylene chloride. The solvent was removed, leaving a blue powder (yield 0.527 g, 0.663 mmol, 64%). IR (KBr): $\nu_{CO}$ 1898 cm$^{-1}$. $^1$H NMR ($\delta$, $CD_2Cl_2$): 7.5−7.2 (m, 5 H, Ph); 6.15, 5.88, 5.72 (3 s, Tp′ C−*H*); 4.06 (dqd, 1 H, $^3J_{HH}$ = 10.2, 6.5, and 3.2 Hz, −C*H*(CH$_3$)(CH$_2$Ph)); 3.65 (dd, 1 H, $^2J_{HH}$ = 13.5 Hz, $^3J_{HH}$ = 3.2 Hz, −CH(CH$_3$)(C*H*HPh)); 2.91, 2.65, 2.60, 2.46, 2.40, 2.36, 1.55 (7 s, 3 H each, Tp′ C*H*$_3$ and C*H*$_3$C≡C); 2.26 (dd, 1 H, $^2J_{HH}$ = 13.5 Hz, $^3J_{HH}$ = 10.2 Hz, −CH(CH$_3$)(CH*H*Ph)); 1.56 (d, 3 H, $^3J_{HH}$ = 6.5 Hz, −CH(C*H*$_3$)(CHHPh)). $^{13}$C NMR ($\delta$, $CD_2Cl_2$): 234.1 (s, *C*O); 211.6, 205.4 (2 s, *C*≡*C*); 155.5, 154.2, 150.1, 145.9, 145.5, 144.5 (6 s, Tp′ *C*−CH$_3$); 140.6, 130.0, 128.5, 126.4 (4 s, Ph); 108.5, 108.2, 107.1 (3 s, Tp′ *C*−H); 44.2, 40.4 (2 s, −*C*H(CH$_3$)(*C*H$_2$Ph)); 20.4, 19.3, 19.2, 18.5, 16.4, 13.0, 12.8, 12.7 (8 s, Tp′ *C*H$_3$ and *C*H$_3$C≡CCH(*C*H$_3$)(CH$_2$Ph)). Anal. Calcd for $C_{28}H_{36}N_6WBOI$: C, 42.35; H, 4.57; N, 10.58. Found: C, 42.83; H, 4.58; N, 10.80.

**Tp′(CO)(I)W{CH$_3$C≡CCH(CH$_2$Ph)Me} (8b)**. To a blue-green solution of Tp′(CO)(I)W{CH$_3$C≡CCH$_2$CH$_2$Ph} (0.736 g, 0.942 mmol) in THF, cooled to −78 °C, was added butyllithium (0.68 mL, 1.70 mmol). To the resulting red-brown solution was added iodomethane (0.59 mL, 9.42 mmol) through a layer of alumina. The color of the solution changed to blue-green over 5 min. The solvent was removed, leaving a blue-green oil. The oil was chromatographed on alumina, and a blue-green band was eluted with methylene chloride. The solvent was removed, leaving a blue-green powder (yield 0.516 g, 0.650 mmol, 69%). IR (KBr): $\nu_{CO}$ 1894 cm$^{-1}$. $^1$H NMR ($\delta$, $CD_2Cl_2$): 7.4−7.2 (m, 5 H, Ph); 6.17, 5.87, 5.76 (3 s, Tp′ C−*H*); 3.99 (dqd, 1 H, $^3J_{HH}$ = 10.9, 7.0, and 3.6 Hz, −C*H*(CH$_2$Ph)(CH$_3$)); 3.53 (dd, 1 H, $^2J_{HH}$ = 13 Hz, $^3J_{HH}$ = 3.6 Hz, −CH(C*H*HPh)(CH$_3$)); 3.18 (dd, 1 H, $^2J_{HH}$ = 13 Hz, $^3J_{HH}$ = 10.9 Hz, −CH(CH*H*Ph)(CH$_3$)); 2.87, 2.78, 2.61, 2.47, 2.38, 2.37, 1.62 (7 s, 3 H each, Tp′ C*H*$_3$ and C*H*$_3$C≡C); 1.29 (d, 3 H, $^3J_{HH}$ = 7.0 Hz, −CH(CHHPh)(C*H*$_3$)). $^{13}$C NMR ($\delta$, $CD_2Cl_2$): 237.2 (s, *C*O); 210.9, 207.5 (2 s, *C*≡*C*); 155.6, 155.5, 150.5, 146.0, 145.7, 144.6 (6 s, Tp′ *C*−CH$_3$); 140.9, 129.6, 128.9, 126.8 (4 s, Ph); 108.6, 108.2, 107.1 (3 s, Tp′ *C*−H); 45.1, 43.7 (2 s, −*C*H(*C*H$_2$Ph)(CH$_3$)); 20.7, 19.2, 18.4, 16.2, 13.2, 13.1, 12.7, 12.6 (8 s, Tp′ *C*H$_3$ and *C*H$_3$C≡CCH(CH$_2$Ph)(*C*H$_3$)). Anal. Calcd for $C_{28}H_{36}N_6WBOI$: C, 42.35; H, 4.57; N, 10.58. Found: C, 42.66; H, 4.58; N, 10.80.

**Tp′(CO)(I)W{CH$_3$CH$_2$C≡CCH$_2$CH$_3$} (9)**. To a red-brown THF solution of Tp′(CO)$_3$IW[20] (2.00 g, 2.89 mmol) was added 3-hexyne (0.394 mL, 3.47 mmol). The solution was refluxed for 24 h. The solvent was removed from the resulting green solution, leaving a dark geen solid. The solid was chromatographed on alumina, and a green band was eluted with methylene chloride. The solvent was removed, leaving a green powder (yield 1.283 g, 1.79 mmol, 62%). IR (KBr): $\nu_{CO}$ 1900 cm$^{-1}$. $^1$H NMR ($\delta$, $CD_2Cl_2$): 6.12, 5.84, 5.69 (3 s, Tp′ C−*H*); 3.94, 3.49 (2 dq, 1 H each, $^2J_{HH}$ = 15.0 Hz, $^3J_{HH}$ = 7.5 Hz, CH$_3$CH$_2$C≡CC*H*$_2$CH$_3$); 3.62, 2.83 (2 dq, 1 H each, $^2J_{HH}$ = 15.1 Hz, $^3J_{HH}$ = 7.6 Hz, CH$_3$C*H*$_2$C≡CCH$_2$CH$_3$); 2.83, 2.57, 2.43, 2.33, 1.52 (5 s, 3:3:3:6:3, Tp′ C*H*$_3$); 1.47 (t, 3 H, $^3J_{HH}$ = 7.5 Hz, CH$_3$CH$_2$C≡CCH$_2$C*H*$_3$); 0.56 (t, 3 H, $^3J_{HH}$ = 7.6 Hz, C*H*$_3$CH$_2$C≡CCH$_2$CH$_3$). $^{13}$C NMR ($\delta$, $CD_2Cl_2$): 233.6 (s, *C*O); 215.4, 203.8 (2 s, *C*≡*C*); 155.3, 154.3, 150.4, 145.8, 145.3, 144.3 (6 s, Tp′ *C*−CH$_3$); 108.3, 108.1, 107.0 (3 s, Tp′ *C*−H); 40.0, 30.0, 28.6, 19.5, 18.3, 16.5, 13.3, 13.0, 12.8, 12.0 (10 s, Tp′ *C*H$_3$ and *C*H$_3$CH$_2$C≡C*C*H$_2$*C*H$_3$). Anal. Calcd for $C_{22}H_{32}N_6WBOI$: C, 36.80; H, 4.49; N, 11.70. Found: C, 36.84; H, 4.49; N, 11.69.

**Tp′(CO)(I)W{CH$_3$CH$_2$C≡CCHMeCH$_2$Ph} (10)**. To a green solution of Tp′(CO)(I)W{CH$_3$CH$_2$C≡CCH$_2$CH$_3$} (0.882 g, 1.23 mmol) in THF, cooled to −78 °C, was added butyllithium (0.59 mL, 1.48 mmol). To the resulting red-brown solution was added benzyl bromide (0.44 mL, 3.68 mmol). The color of the solution changed to blue-green over 30 min. The solvent was removed, leaving a dark green oil. The oil was chromatographed on alumina, and a green band was eluted with methylene chloride. The solvent was removed, leaving a green solid. The solid was taken up in methylene chloride and

layered with hexanes to obtain the green crystals (yield 0.607 g, 0.75 mmol, 61%). IR (KBr): $\nu_{CO}$ 1893 cm$^{-1}$. $^1$H NMR ($\delta$, $CD_2Cl_2$): 7.4−7.2 (m, 5 H, Ph); 6.13, 5.86, 5.70 (3 s, Tp′ C−*H*); 4.12 (dqd, 1 H, $^3J_{HH}$ = 10.2, 6.7, and 3.4 Hz, −C*H*(CH$_3$)(CH$_2$Ph)); 3.78 (dq, 1 H, $^2J_{HH}$ = 14.9 Hz, $^3J_{HH}$ = 7.5 Hz, CH$_3$C*H*H−); 3.59 (dd, 1 H, $^2J_{HH}$ = 13.4 Hz, $^3J_{HH}$ = 3.4 Hz, −CH(CH$_3$)(C*H*HPh)); 2.93 (dq, 1 H, $^2J_{HH}$ = 14.9 Hz, $^3J_{HH}$ = 7.5 Hz, CH$_3$CH*H*−); 2.88, 2.59, 2.44, 2.35, 2.34, 1.60 (6 s, 3 H each, Tp′ C*H*$_3$); 2.25 (dd, 1 H, $^2J_{HH}$ = 13.4 Hz, $^3J_{HH}$ = 10.2 Hz, −CH(CH$_3$)(CH*H*Ph)); 1.57 (d, 3 H, $^3J_{HH}$ = 6.7 Hz, −CH(C*H*$_3$)(CH$_2$Ph)); 0.27 (t, 3 H, $^3J_{HH}$ = 7.6 Hz, C*H*$_3$CHH−). $^{13}$C NMR ($\delta$, $CD_2Cl_2$): 234.2 (s, *C*O); 214.8, 203.2 (2 s, *C*≡*C*); 155.3, 154.3, 150.8, 146.1, 145.4, 144.4 (6 s, Tp′ *C*−CH$_3$); 140.6, 130.0, 128.5, 126.4 (4 s, Ph); 108.5, 108.1, 106.9 (3 s, Tp′ *C*−H); 44.1, 40.5 (2 s, *C*H(CH$_3$)(*C*H$_2$Ph)); 28.2, 19.8, 19.7, 18.5, 16.7, 13.0, 12.9, 12.8, 11.7 (9 s, Tp′ *C*H$_3$ and *C*H$_3$*C*H$_2$C≡CCH(*C*H$_3$)(CH$_2$Ph)). Anal. Calcd for $C_{29}H_{38}N_6WBOI$: C, 43.10; H, 4.74; N, 10.40. Found: C, 43.33; H, 4.66; N, 10.21.

**Tp′(CO)(I)W{Me(PhCH$_2$)HCC≡CCHMeCH(OH)Ph} (11)**. A green THF solution of Tp′(CO)(I)W{CH$_3$CH$_2$C≡CCHMeCH$_2$Ph} (0.810 g, 1.00 mmol) was refluxed for 48 h to form a 2:3 ratio (by $^1$H NMR) of the two isomers Tp′(CO)(I)W{CH$_3$CH$_2$C≡CCHMeCH$_2$Ph} and Tp′(CO)(I)W{Me(PhCH$_2$)HCC≡CCH$_2$CH$_3$} (0.60 and 0.40 mmol). This mixture of isomers in THF was cooled to −78 °C, and butyllithium (0.40 mL, 1.00 mmol) was added. To the resulting brown-green solution was added benzaldehyde (0.51 mL, 5.00 mmol). The color of the solution changed to green immediately. The reaction was quenched by the addition of HCl (1.10 mL of 1.0 M HCl in diethyl ether, 1.10 mmol). The solvent was removed, leaving a green oil. The oil was chromatographed on alumina, and a green band was eluted with methylene chloride. The solvent was removed, leaving a green solid, which was determined by $^1$H NMR to be starting material. A second green band was eluted with a mixture of THF and methanol. The solvent was removed, leaving a green oil. The oil was taken up in methylene chloride and layered with hexanes to obtain green crystals (yield 0.130 g, 0.142 mmol, 14%). IR (KBr): $\nu_{CO}$ 1910 cm$^{-1}$. $^1$H NMR ($\delta$, $CD_2Cl_2$): 7.6−7.1, 6.6−6.5 (m, 10 H, Ph); 6.22, 5.88, 5.68 (3 s, Tp′ C−*H*); 4.85 (dd, 1 H, $^2J_{HH}$ = 7.5 Hz, $^3J_{HH}$ = 3 Hz, −CHMeC*H*(OH)Ph); 4.61 (dq, 1 H, $^3J_{HH}$ = 6.9 Hz, $^3J_{HH}$ = 6.8 Hz, −C*H*MeCH(OH)Ph); 3.69 (m, 1 H, (CH$_3$)(PhCH$_2$)*H*C−); 2.89, 2.69, 2.45, 2.36, 2.35, 1.74 (6 s, 3 H each, Tp′ C*H*$_3$); 2.80 (d, 1 H, $^3J_{HH}$ = 3 Hz, −CHMeCH(O*H*)Ph); 1.45 (d, 3 H, $^3J_{HH}$ = 6.8 Hz, −CH(C*H*$_3$)CH(OH)Ph); 1.45, 1.13 (2 dd, 1 H each, coupling obscured by methyl doublets, (CH$_3$)(PhC*H*H)HC−); 1.09 (d, 3 H, $^3J_{HH}$ = 6.7 Hz, (C*H*$_3$)(PhCH$_2$)HC−). $^{13}$C NMR ($\delta$, $CD_2Cl_2$): 233.6 (s, *C*O); 219.6, 201.5 (2 s, *C*≡*C*); 155.3, 154.6, 151.9, 147.1, 145.6, 144.7 (6 s, Tp′ *C*−CH$_3$); 142.2, 140.3, 129.2, 128.5, 128.4, 128.1, 127.9, 126.3 (8 s, Ph); 109.0, 108.1, 107.4 (3 s, Tp′ *C*−H); 78.7 (s, −CH(CH$_3$)(*C*H(OH)Ph)); 49.6, 42.6, 38.6 (3 s, (CH$_3$)(Ph*C*H$_2$)H*C*−, −*C*H(CH$_3$)(CH(OH)Ph)); 20.3, 20.2, 19.8, 18.6, 16.9, 13.1, 12.8, 12.7 (8 s, Tp′ *C*H$_3$ and (*C*H$_3$)(PhCH$_2$)HC−, −CH(*C*H$_3$)(CH(OH)Ph)). Anal. Calcd for $C_{36}H_{44}N_6WBO_2I$: C, 46.59; H, 4.91; N, 9.31. Found: C, 46.81; H, 4.83; N, 9.14.

**[Tp′(CO)$_2$W{CH$_3$C≡CCH$_3$}][OTf] (12)**. Silver triflate (12.25 g, 47.7 mmol) was added to a red-brown solution of Tp′(CO)$_3$IW (30.005 g, 43.4 mmol) and 2-butyne (13.5 mL, 173 mmol) in methylene chloride. The color of the solution changed to green, and a gray precipitate formed after 1.5 h. The green solution was filtered away from the precipitate. The solvent was removed, leaving a green oil. The oil was washed with 100 mL of diethyl ether. The brown ether wash was filtered away, leaving a blue-green solid. A methylene chloride solution of the blue-green solid was passed through a Celite column. The blue-green solid resulting from removal of the solvent was recrystallized from methylene chloride and hexanes, yielding a blue-green powder (yield 26.617 g, 36.0 mmol, 83%). IR (KBr): $\nu_{CO}$ 2068, 1979 cm$^{-1}$. $^1$H NMR ($\delta$, $CD_2Cl_2$): 6.12, 6.06 (2 s, 1:2 H, Tp′ C−*H*); 3.63, 2.86 (2 broad s, 3:3 H, C*H*$_3$C≡CC*H*$_3$); 2.64, 2.59, 2.43, 1.59 (4 s, 3:6:3:6 H, Tp′ C−C*H*$_3$). $^{13}$C NMR ($\delta$, $CD_2Cl_2$): 236.5, 205.2 (2 broad s, *C*≡*C*) 217.6 (s, *C*O); 156.0, 151.3, 150.6, 147.5 (4 s, 1:2:1:2, Tp′ *C*−CH$_3$); 121.4 (q, $^1J_{CF}$ = 320 Hz, −O$_3$S*C*F$_3$); 110.0, 108.6 (2 s, 1:2, Tp′ *C*−H); 24.2, 23.6 (2 broad s, *C*H$_3$C≡C*C*H$_3$); 16.3, 15.8, 13.3, 12.7 (4 s, 1:2:1:2, Tp′ *C*H$_3$). Anal. Calcd for $C_{22}H_{28}N_6WBO_5SF_3I$: C, 35.70; H, 3.81; N, 11.35. Found: C, 35.60; H, 3.83; N, 11.34.

**Tp′(CO)(OTf)W{CH$_3$C≡CCH$_3$} (13)**. This complex was prepared by two methods.

**Method A.** To a green solution of Tp′(CO)(I)W{CH$_3$C≡CCH$_3$} (6.00 g, 8.68 mmol) in THF, cooled to 0 °C, was added silver triflate (2.435 g, 9.55 mmol). The color changed to blue with a gray precipitate after 1.5 h of stirring at 0 °C. The blue solution was filtered into hexanes, producing a blue precipitate. The solvent was removed, yielding a blue powder (yield 5.679 g, 7.973 mmol, 92%).

**Method B.** A blue-green slurry of [Tp′(CO)$_2$W{CH$_3$C≡CCH$_3$}][OTf] (24.055 g, 32.5 mmol) in THF was refluxed for 2 h. The color of the solution changed to blue. A blue solid was obtained by removing the solvent. The solid was eluted through an alumina column with methylene chloride. The blue solid obtained by removing the solvent was recrystallized from methylene chloride and hexanes, yielding blue crystals (yield 15.350 g, 21.57 mmol, 67%). IR (KBr): $\nu_{CO}$ 1913 cm$^{-1}$. $^1$H NMR ($\delta$, $CD_2Cl_2$): 6.05, 5.95, 5.76 (3 s, Tp′ C−*H*); 3.59, 2.91 (2 s, 3:3 H, C*H*$_3$C≡CC*H*$_3$); 2.65, 2.54, 2.48, 2.40, 1.98, 1.45 (6 s, 3 H each, Tp′ C−C*H*$_3$). $^{13}$C NMR ($\delta$, $CD_2Cl_2$): 230.3 (s, *C*O); 211.1, 204.2 (2 s, *C*≡*C*) 154.8, 152.8, 151.1, 147.2, 146.6, 145.0 (6 s, Tp′ *C*−CH$_3$); 119.9 (q, $^1J_{CF}$ = 318 Hz, −O$_3$S*C*F$_3$); 108.1, 108.0, 107.6 (3 s, Tp′ *C*−H);) 21.7, 19.4, 16.0, 15.1, 14.0, 12.9, 12.8, 12.7 (8 s, Tp′ *C*H$_3$ and *C*H$_3$C≡C*C*H$_3$). Anal. Calcd for $C_{22}H_{28}N_6WBO_5SF_3I$: C, 35.42; H, 3.96; N, 11.80. Found: C, 35.41; H, 4.00; N, 11.86.

**Synthesis of ($S_W$,$S_C$)-(+)- and ($R_W$,$S_C$)-(−)-Tp′(CO)W{CH$_3$C≡CCH$_3$}(NHR) (R = (*S*)-(−)-α-methylbenzyl) ((−)-14(*RS*), (+)-14(*SS*)).** A blue solution of Tp′(CO)(OTf)W{CH$_3$C≡CCH$_3$} (14.263 g, 19.3 mmol) and (*S*)-NH$_2$CHMePh (7.70 mL, 59.7 mmol) in THF was refluxed for 36 h. The color of the solution changed to orange. An orange solid was obtained by removing the solvent. The solid was eluted through an alumina column with a 1:1 mixture of methylene chloride and hexanes. An orange solid was obtained by removing the solvent. The presence of a 1:1 mixture of **(−)-14(*RS*)** and **(+)-14(*SS*)** was confirmed by $^1$H NMR (yield 12.89 g, 18.9 mmol, 97%).

**Separation of the Diastereomers of ($S_W$,$S_C$)-(+)- and ($R_W$,$S_C$)-(−)-Tp′(CO)W{CH$_3$C≡CCH$_3$}(NHR) (R = (*S*)-(−)-α-Methylbenzyl; (−)-14(*RS*), (+)-14(*SS*)).** A 1:1 mixture of **(−)-14(*RS*)** and **(+)-14(*SS*)** (5.506 g, 8.06 mmol) was dissolved in methylene chloride and the solution layered with pentane. Orange crystals were formed, which were determined to be a single diastereomer by $^1$H NMR. Three more crops of crystals were grown in the same manner, and all were determined to be a single diastereomer by $^1$H NMR. The four crops of the single-diastereomer crystals were combined (yield 1.72 g, 2.52 mmol, 31%). This diastereomer was confirmed to be **(+)-14(*SS*)** by X-ray crystallography (see below). The second isomer remained in solution and was isolated by evaporation (4:1 mixture of **(−)-14(*RS*)** and **(+)-14(*SS*)**). **(−)-14(*RS*)** could not be crystallized, but a pure sample was obtained by deprotonation of **(−)-15(*RS*)** with BuLi in THF at −78°C.

**($S_W$,$S_C$)-(+)-Tp′(CO)W{CH$_3$C≡CCH$_3$}(NHR) ((+)-14(*SS*)).** $[\alpha]^{25}_{589}$ = +110° ($c$ = 4.6 × 10$^{-4}$ g/mL in $CH_2Cl_2$). IR (KBr): $\nu_{CO}$ 1839 cm$^{-1}$. $^1$H NMR ($\delta$, $CD_2Cl_2$): 7.21−6.80 (m, 5 H, Ph); 6.56 (d, 1 H, $^3J_{HH}$ = 9.0 Hz, N*H*); 6.11, 5.87, 5.53 (3 s, Tp′ C−*H*); 5.45 (qd, 1 H, $^3J_{HH}$ = 9.0 Hz, $^3J_{HH}$ = 7.0 Hz, NHC*H*(CH$_3$)Ph); 2.85, 2.51, 2.33, 2.30, 2.29, 2.22, 2.14, 1.53 (8 s, 3 H each, Tp′ C−C*H*$_3$ and C*H*$_3$C≡CC*H*$_3$); 1.22 (d, 3 H, $^3J_{HH}$ = 7.0 Hz, NHCH(C*H*$_3$)Ph). $^{13}$C NMR ($\delta$, $CD_2Cl_2$): 239.0 (s, *C*O); 169.4, 161.9 (2 s, *C*≡*C*); 153.7, 150.6, 150.5, 149.9, 144.7, 144.5, 144.1 (7 s, Tp′ *C*−CH$_3$ and ipso C of Ph); 128.3, 126.8, 125.9 (3 s, Ph); 108.1, 107.3, 106.3 (3 s, Tp′ *C*−H); 71.5 (s, NHC*H*(CH$_3$)Ph);

28.2, 16.2, 15.7, 15.6, 15.5, 14.5, 13.0, 12.9, 12.7 (9 s, Tp′ *C*H$_3$, *C*H$_3$C≡C*C*H$_3$, and NHCH(*C*H$_3$)Ph). Anal. Calcd for $C_{28}H_{38}N_7$WBO: C, 49.22; H, 5.61; N, 14.35. Found: C, 49.33; H, 5.53; N, 14.29.

**($R_W$,$S_C$)-(−)-Tp′(CO)W{CH$_3$C≡CCH$_3$}(NHR) ((−)-14(*RS*)).** $[\alpha]^{25}_{589} = -340°$ ($c = 5.0 \times 10^{-4}$ g/mL in $CH_2Cl_2$). IR (KBr): $\nu_{CO}$ 1838 cm$^{-1}$. $^1$H NMR ($\delta$, $CD_2Cl_2$): 7.3−7.0 (m, 5 H, Ph); 6.67 (d, 1 H, $^3J_{HH}$ = 10 Hz, N*H*); 6.07, 5.68, 5.57 (3 s, Tp′ C−*H*); 5.38 (qd, 1 H, $^3J_{HH}$ = 10 Hz, $^3J_{HH}$ = 6 Hz, NHC*H*(CH$_3$)Ph); 3.02, 2.50, 2.49, 2.30, 2.29, 2.27, 2.26, 1.66 (8 s, 3 H each, Tp′ C−C*H*$_3$ and C*H*$_3$C≡CC*H*$_3$); 0.87 (d, 3 H, $^3J_{HH}$ = 10 Hz, NHCH(C*H*$_3$)Ph). $^{13}$C NMR ($\delta$, $CD_2Cl_2$): 239.0 (s, *C*O); 168.6, 159.0 (2 s, *C*≡*C*); 153.2, 150.5, 150.3, 150.1, 144.4, 144.1, 144.0 (7 s, Tp′ *C*−CH$_3$ and ipso C of Ph); 128.5, 126.2, 125.8 (3 s, Ph); 107.9, 106.8, 106.1 (3 s, Tp′ *C*−H); 72.5 (s, NH*C*H(CH$_3$)Ph); 26.7, 17.4, 15.8, 15.6, 15.5, 14.5, 12.9, 12.8, 12.7 (9 s, Tp′ *C*H$_3$, *C*H$_3$C≡C*C*H$_3$, and NHCH(*C*H$_3$)Ph). Anal. Calcd for $C_{28}H_{38}N_7$WBO: C, 49.22; H, 5.61; N, 14.35. Found: C, 49.36; H, 5.58; N, 14.59.

**($S_W$,$S_C$)-(+)-[Tp′(CO)W{CH$_3$C≡CCH$_3$}(NH$_2$R)][BF$_4$] (R = (*S*)-(−)-α-Methylbenzyl; (+)-15(*SS*))**. To an orange methylene chloride solution of $S_WS_C$-(+)-Tp′(CO)W{CH$_3$C≡CCH$_3$}(NHR) (6.572 g, 9.62 mmol) was added HBF$_4$·OMe$_2$ (1.17 mL, 9.6 mmol). The resulting purple solution was transferred via cannula into diethyl ether, producing a purple precipitate. The supernatant was filtered away, and the residual solvent was removed, leaving a purple powder (7.597 g, 9.37 mmol, 97%). $[\alpha]^{25}_{589} = +520°$ ($c = 5.0 \times 10^{-4}$ g/mL in $CH_2Cl_2$). IR (KBr): $\nu_{CO}$ 1902 cm$^{-1}$. $^1$H NMR ($\delta$, $CD_2Cl_2$): 7.5−7.1 (m, 5 H, Ph); 6.15, 6.12, 5.78 (3 s, Tp′ C−*H*); 3.90, 3.40 (2 m, 1:2 H, *H*N*HCH*(CH$_3$)Ph); 3.42, 2.97, 2.85, 2.53, 2.43, 2.41, 1.99, 1.42 (8 s, 3 H each, Tp′ C−C*H*$_3$ and C*H*$_3$C≡CC*H*$_3$); 1.70 (d, 3 H, $^3J_{HH}$ = 7 Hz, NHHCH(C*H*$_3$)Ph). $^{13}$C NMR ($\delta$, $CD_2Cl_2$): 231.5 (s, *C*O); 221.0, 212.4 (2 s, *C*≡*C*); 152.9, 151.3, 150.9, 148.0, 147.5, 146.5 (6 s, Tp′ *C*−CH$_3$); 141.8, 129.7, 129.3, 125.9 (4 s, Ph); 109.5, 109.2, 108.0 (3 s, Tp′ *C*−H); 62.5 (s, NH$_2$*C*H(CH$_3$)Ph); 24.1, 22.0, 20.7, 16.0, 15.9, 14.9, 13.0, 12.9, 12.7 (9 s, Tp′ *C*H$_3$, *C*H$_3$C≡C*C*H$_3$, and NH$_2$CH(*C*H$_3$)Ph). Anal. Calcd for $C_{28}H_{39}N_7WB_2OF_4$: C, 43.61; H, 5.10; N, 12.71. Found: C, 43.66; H, 5.16; N, 12.74.

**($R_W$,$S_C$)-(−)-[Tp′(CO)W{CH$_3$C≡CCH$_3$}(NH$_2$R)][BF$_4$] (R = (*S*)-(−)-α-Methylbenzyl; (−)-15(*RS*))**. The procedure for protonation of **(−)-14(*RS*)** (1.50 g, 2.20 mmol) was the same as that described above. Purple crystals of a single diastereomer were obtained from methylene chloride and diethyl ether (1.21 g, 1.57 mmol, 71%). $[\alpha]^{25}_{589} = -280°$ ($c = 5.1 \times 10^{-4}$ g/mL in $CH_2Cl_2$). IR (KBr): $\nu_{CO}$ 1906 cm$^{-1}$. $^1$H NMR ($\delta$, $CD_2Cl_2$): 7.5−7.1 (m, 5 H, Ph); 6.27, 5.95, 5.76 (3 s, 3 H each, Tp′ C−*H*); 4.12, 3.87, 3.15 (3 m, 1 H each, *H*N*HCH*(CH$_3$)Ph); 3.63, 3.07, 2.54, 2.42, 2.41, 2.36, 2.35, 1.42 (8 s, 3 H each, Tp′ C−C*H*$_3$ and C*H*$_3$C≡CC*H*$_3$); 1.05 (d, 3 H, $^3J_{HH}$ = 7 Hz, NHHCH(C*H*$_3$)Ph). $^{13}$C NMR ($\delta$, $CD_2Cl_2$): 230.6 (s, *C*O); 221.7, 212.3 (2 s, *C*≡*C*); 153.0, 151.3, 150.7, 148.0, 147.7, 146.7 (6 s, Tp′ *C*−CH$_3$); 142.1, 129.9, 129.7, 126.1 (4 s, Ph); 109.4, 109.3, 108.0 (3 s, Tp′ *C*−H); 63.5 (s, NH$_2$*C*H(CH$_3$)Ph); 22.6, 22.3, 20.8, 16.0, 15.8, 15.1, 12.9, 12.8, 12.7 (9 s, Tp′ *C*H$_3$, *C*H$_3$C≡C*C*H$_3$, and NH$_2$-CH(*C*H$_3$)Ph). Anal. Calcd for $C_{28}H_{39}N_7WB_2OF_4$: C, 43.61; H, 5.10; N, 12.71. Found: C, 43.87; H, 5.28; N, 12.79.

**(+)-Tp′(CO)(I)W{CH$_3$C≡CCH$_3$} ((+)-1).** A purple THF solution of (+)-[Tp′(CO)W{CH$_3$C≡CCH$_3$}(NH$_2$R)][BF$_4$] **((+)-15-(*SS*)**; 3.432 g, 4.23 mmol), [Bu$^n_4$N][I] (4.707 g, 12.7 mmol), and HBF$_4$·OEt$_2$ (0.31 mL, 2.1 mmol) was refluxed for 20 h. The solution was cooled, and another portion of HBF$_4$·OEt$_2$ (0.31 mL, 2.1 mmol) was added. The solution was refluxed for an additional 6.5 h. The solvent was removed from the green solution. The resulting green solid was eluted through an alumina column with a 1:1 mixture of hexanes and methylene chloride. The green solid obtained by removing the solvent was recrystallized from methylene chloride and hexanes, yielding green crystals (yield 2.101 g, 3.04 mmol, 72%). $[\alpha]^{25}_{589} = +740°$ ($c = 4.6 \times 10^{-4}$ g/mL in $CH_2Cl_2$).

**(+)-Tp′(CO)(I)W{CH$_3$C≡CCH$_2$CH$_3$} ((+)-2).** A portion of (+)-Tp′(CO)(I)W{CH$_3$C≡CCH$_3$} (0.300 g, 0.43 mmol) was methylated in a procedure analogous to the racemic complex. A green powder (0.197 g, 0.28 mmol, 65%) was obtained. $[\alpha]^{25}_{589} = +730°$ ($c = 4.6 \times 10^{-4}$ g/mL in $CH_2Cl_2$).

**(+)-Tp′(CO)(I)W{CH$_3$C≡CCHMeCH$_2$Ph} ((+)-8a).** To a green solution of (+)-Tp′(CO)(I)W{CH$_3$C≡CCH$_3$} (0.466 g, 0.675 mmol) in THF, cooled to −78 °C, was added butyllithium (0.41 mL, 1.0 mmol). To the resulting red-brown solution was added iodomethane (0.42 mL, 6.75 mmol). The color of the solution immediately changed to green. The solvent was removed, leaving a green oil. The oil was chromatographed on alumina, and a green band was eluted with methylene chloride. The solvent was removed, leaving a green solid, presumably (+)-Tp′(CO)(I)W{CH$_3$C≡CCH$_2$CH$_3$}. This solid was dissolved in THF, the solution was cooled to −78 °C, and butyllithium (0.41 mL, 1.0 mmol) was added. To the resulting red-brown solution was added benzyl bromide (0.231 g, 1.35 mmol). The color of the solution changed to blue-green over 30 min. The solvent was removed, leaving a blue-green oil. The oil was chromatographed on alumina, and a blue-green band was eluted with methylene chloride. The solvent was removed, leaving a blue solid (0.300 g, 0.378 mmol, 56%). $[\alpha]^{25}_{589} = +850°$ ($c = 5.7 \times 10^{-4}$ g/mL in $CH_2Cl_2$).

**(−)-Tp′(CO)(I)W{CH$_3$C≡CCH$_3$} ((−)-1).** A portion of **(−)-15(*RS*)** (0.560 g, 0.727 mmol) was converted to (−)-Tp′(CO)-(I)W{CH$_3$C≡CCH$_3$} (0.303 g, 0.439 mmol, 60%) (green powder) using a procedure analogous to the synthesis of the other enantiomer. $[\alpha]^{25}_{589} = -730°$ ($c = 4.6 \times 10^{-4}$ g/mL in $CH_2Cl_2$).

**(−)-Tp′(CO)(I)W{CH$_3$C≡CCH$_2$CH$_3$} ((−)-2).** A portion of (−)-Tp′(CO)(I)W{CH$_3$C≡CCH$_3$} **((−)-1**; 0.303 g, 0.439 mmol) was methylated in a procedure analogous to the racemic complex. A green powder (yield 0.215 g, 0.305 mmol, 69%) was obtained. $[\alpha]^{25}_{589} = -740°$ ($c = 4.6 \times 10^{-4}$ g/mL in $CH_2Cl_2$).

**(−)-Tp′(CO)(I)W{CH$_3$C≡CCHMeCH$_2$Ph} ((−)-8a).** A portion of (−)-Tp′(CO)(I)W{CH$_3$C≡CCH$_2$CH$_3$} **((−)-2**; 0.196 g, 0.278 mmol) was benzylated in a procedure analogous to the racemic complex. A light blue powder (yield 0.0915 g, 0.115 mmol, 41%) was obtained. $[\alpha]^{25}_{589} = -850°$ ($c = 5.7 \times 10^{-4}$ g/mL in $CH_2Cl_2$).

**Isolation of Free Alkynes. PhC≡CCH$_3$.** A 150 mL THF solution of Tp′(CO)(I)W{PhC≡CCH$_3$} (0.710 g, 0.944 mmol) was photolyzed for 2 h with air bubbling through the solution in a Schlenk tube fitted with a condenser. The green solution became red-brown during the photolysis, and no carbonyl stretch was evident in the IR spectrum. The solvent was removed to near-dryness, leaving a brown oily solid. The free alkyne was extracted from the solid with pentane. The pentane solution was passed through a column that consisted of a layer of Celite on top of a layer of alumina. The pentane was removed, yielding a colorless oil (0.0968 g, 0.835 mmol, 88%)

**Racemic CH$_3$C≡CCHMeCH$_2$Ph.** A 200 mL THF solution of racemic Tp′(CO)(I)W{CH$_3$C≡CCHMeCH$_2$Ph} (**8a**; 0.969 g, 1.22 mmol) was photolyzed for 1 h with air bubbling through the solution. The blue solution became golden brown during the photolysis, and no carbonyl stretch was evident in the IR spectrum. The solvent was removed to near-dryness, leaving a brown oily solid. The CH$_3$C≡CCHMeCH$_2$Ph was extracted from the solid with hexane. The hexane solution was passed through a column that consisted of a layer of Celite on top of a layer of alumina. The hexane was removed, yielding a slightly yellow oil (0.164 g, 1.04 mmol, 85%) which was determined to be pure by GC and $^1$H and $^{13}$C NMR. $^1$H NMR ($CDCl_3$): $\delta$ 7.35−6.15 (m, 5 H, Ph); 2.70 (m, 3 H, CH$_3$C≡CC*H*MeC*H*$_2$Ph); 1.75 (d, 3 H, $^5J_{HH}$ = 2.2 Hz, C*H*$_3$C≡CCHMeCH$_2$Ph); 1.13 (d, 3 H, $^3J_{HH}$ = 6.6 Hz, CH$_3$C≡CCH(C*H*$_3$)CH$_2$Ph). $^{13}$C NMR ($CDCl_3$): $\delta$ 140.5 (s, ipso C of Ph); 129.6, 128.4, 126.4 (3 s, Ph); 83.5, 76.7 (2 s, *C*≡*C*); 43.8 (1 s, CH$_3$C≡C*C*HMeCH$_2$Ph); 28.4 (1 s, CH$_3$C≡CCHMe*C*H$_2$Ph); 21.2 (1 s, CH$_3$C≡CCH(*C*H$_3$)CH$_2$Ph); 3.5 (1 s, *C*H$_3$C≡CCHMeCH$_2$Ph).

**(−)-$CH_3C{\equiv}CCHMeCH_2Ph$.** The optically pure alkyne (−)-$CH_3C{\equiv}CCHMeCH_2Ph$ (0.0484 g, 0.306 mmol, 81%) was obtained as a colorless oil from (+)-Tp′(CO)(I)W{$CH_3C{\equiv}CCHMeCH_2Ph$} (**(+)-8a**; 0.300 g, 0.378 mmol) using the same procedure as for the racemic analogue. $[\alpha]^{25}_{589} = -56°$ ($c = 4.8 \times 10^{-4}$ g/mL in $CH_2Cl_2$).

**(+)-$CH_3C{\equiv}CCHMeCH_2Ph$.** The optically pure alkyne (+)-$CH_3C{\equiv}CCHMeCH_2Ph$ (0.0069 g, 0.044 mmol, 42%) was obtained as a colorless oil from (−)-Tp′(CO)(I)W{$CH_3C{\equiv}CCHMeCH_2Ph$} (**(−)-8a**; 0.083 g, 0.104 mmol) using the same procedure as for the racemic analogue. $[\alpha]^{25}_{589} = +39°$ ($c = 6.9 \times 10^{-3}$ g/mL in $CH_2Cl_2$). $[\alpha]^{25}_{589} = +64°$ ($c = 2.2 \times 10^{-3}$ g/mL in $CH_2Cl_2$).

**Photolytic Tungsten−Alkyne Cleavage Yields by Gas Chromatography (Alkyne = $CH_3C{\equiv}CCH_3$, $CH_3C{\equiv}CCH_2CH_3$, $PhC{\equiv}CCH_3$, $PhC{\equiv}CCH_2CH_3$).** The complexes Tp′(CO)(I)W{$CH_3C{\equiv}CCH_3$} (**1**; 0.0806 g, 1.17 mmol), Tp′(CO)(I)W{$CH_3C{\equiv}CCH_2CH_3$} (**2**; 0.0821 g, 1.17 mmol), Tp′(CO)(I)W{$PhC{\equiv}CCH_3$} (0.0881 g, 1.17 mmol), and Tp′(CO)(I)W{$PhC{\equiv}CCH_2CH_3$} (0.0897 g, 1.17 mmol) with nonane (0.0208 mL, 0.117 mmol) added to each as an internal standard were diluted with THF to 25.00 mL in separate volumetric flasks in air. The solutions were sealed and photolyzed for 2 h. The color of each solution changed from green to red-brown, and no CO stretch was evident in the infrared spectra. Gas chromatograms were made of each reaction mixture. The chromatograms were compared with those obtained from standard solutions made by diluting nonane (0.0208 mL, 0.117 mmol) with $CH_3C{\equiv}CCH_3$ (0.0091 mL, 1.2 mmol), $CH_3C{\equiv}CCH_2CH_3$ (0.0112 mL, 1.17 mmol), $PhC{\equiv}CCH_3$ (0.0146 mL, 1.17 mmol), and $PhC{\equiv}CCH_2CH_3$ (0.0166 mL, 1.17 mmol) to 25.00 mL with THF. It was determined by comparison with the internal standard that 92%, 97%, 88%, and 82% of $CH_3C{\equiv}CCH_3$, $CH_3C{\equiv}CCH_2CH_3$, $PhC{\equiv}CCH_3$, and $PhC{\equiv}CCH_2CH_3$, respectively, had been liberated from the metal.

**$^1$H NMR Chiral Shift Experiments. Racemic $CH_3C{\equiv}CCHMeCH_2Ph$.** To a 1.0 mL solution of racemic $CH_3C{\equiv}CCHMeCH_2Ph$ (6.8 mg, 0.043 mmol) in $CDCl_3$ were added $Eu(tfc)_3$ (38 mg, 0.043 mmol) and Ag(fod) (17 mg, 0.043 mmol). The doublet at 1.8 ppm was resolved into two broad signals with a 1:1 integral ratio, and the doublet at 1.1 ppm was resolved into two doublets with a 1:1 integral ratio. Other signals were not resolved.

**(−)-$CH_3C{\equiv}CCHMeCH_2Ph$.** Three 1.0 mL samples of (−)-$CH_3C{\equiv}CCHMeCH_2Ph$ (4.8 mg, 0.031 mmol) in $CDCl_3$ were prepared. The following amounts of shift reagents were added to the three samples: (sample 1) $Eu(tfc)_3$ (14 mg, 0.015 mmol) and Ag(fod) (6 mg, 0.015 mmol); (sample 2) $Eu(tfc)_3$ (27 mg, 0.031 mmol) and Ag(fod) (12 mg, 0.031 mmol); (sample 3) $Eu(tfc)_3$ (55 mg, 0.061 mmol) and Ag(fod) (25 mg, 0.061 mmol). No signals due to the presence of a second isomer were evident in the spectra obtained of these three samples.

**Scalemic $CH_3C{\equiv}CCHMeCH_2Ph$.** A 1.0 mL sample in $CDCl_3$ which contained a 7:3 ratio of (−)-$CH_3C{\equiv}CCHMeCH_2Ph$ and (+)-$CH_3C{\equiv}CCHMeCH_2Ph$ was prepared using racemic $CH_3C{\equiv}CCHMeCH_2Ph$ (3.5 mg, 0.022 mmol) and (−)-$CH_3C{\equiv}CCHMeCH_2Ph$ (2.4 mg, 0.015 mmol). To this sample were added $Eu(tfc)_3$ (27 mg, 0.031 mmol) and Ag(fod) (12 mg, 0.031 mmol). The doublet at 1.8 ppm was resolved into two broad signals that were integrated in a 7:3 ratio. The doublet at 1.1 ppm was broadened.

A second 1.0 mL scalemic sample in $CDCl_3$ which contained a 9:1 ratio of (−)-$CH_3C{\equiv}CCHMeCH_2Ph$ to (+)-$CH_3C{\equiv}CCHMeCH_2Ph$ was prepared using racemic $CH_3C{\equiv}CCHMeCH_2Ph$ (1.0 mg, 0.0064 mmol) and (−)-$CH_3C{\equiv}CCHMeCH_2Ph$ (4.1 mg, 0.026 mmol). To this sample were added $Eu(tfc)_3$ (27 mg, 0.031 mmol) and Ag(fod) (12 mg, 0.031 mmol). The doublet at 1.8 ppm in the $^1$H NMR spectrum was resolved into two broad singlets that were integrated in a 9:1 ratio. The doublet at 1.1 ppm was broadened.

**Table 6. Parameters Used in Extended Hückel Calculations**

| atom | orbital | $H_{ii}$ (eV) | $\zeta_1$ | $\zeta_2$ | $C_1$ | $C_2$ |
|---|---|---|---|---|---|---|
| W | 5d | 10.37 | 4.982 | 2.068 | 0.6940 | 0.5631 |
| | 6p | 5.17 | 2.309 | | | |
| | 6s | 8.26 | 2.341 | | | |
| C | 2p | 11.40 | 1.625 | | | |
| | 2s | 21.40 | 1.625 | | | |
| O | 2p | 14.80 | 2.275 | | | |
| | 2s | 32.30 | 2.275 | | | |
| H | 1s | 13.60 | 1.300 | | | |
| N | 2p | 13.40 | 1.950 | | | |
| | 2s | 26.00 | 1.959 | | | |
| I | 5p | 12.70 | 2.322 | | | |
| | 5s | 18.00 | 2.679 | | | |

**Variable-Temperature $^1$H NMR Experiments. Tp′(CO)(I)W{$CH_3C{\equiv}C(CH_2)_4I$} (4).** A sealed-tube NMR sample of Tp′(CO)(I)W{$CH_3C{\equiv}C(CH_2)_4I$} in $d_5$-bromobenzene was prepared. Spectra were recorded at 20, 100, 110, and 120 °C. Coalescence was not achieved. Line widths at half peak height ($\omega_{1/2}$) were measured for the methyl singlet. The natural line width was subtracted from the measured line widths to give the corrected line widths ($\delta\nu$). The rate constant for site exchange ($k_{ex}$) was calculated from the slow exchange approximation $k_{ex} = \pi(\delta\nu)$.[21] The barrier to alkyne rotation ($\Delta G^{\ddagger}$) was calculated from the Eyring equation ($k_{ex} = (kT/h)\exp(-\Delta G^{\ddagger}/RT)$) at 100, 110, and 120 °C to be 20.4, 20.8, and 20.8 kcal/mol, respectively.

**Tp′(CO)(I)W{$CH_3C{\equiv}CCH_3$} (1).** A variable-temperature $^1$H NMR experiment identical with the experiment on Tp′(CO)(I)W{$CH_3C{\equiv}C(CH_2)_4I$} was performed on Tp′(CO)(I)W{$CH_3C{\equiv}CCH_3$}. No significant line broadening was observed at any temperature up to 120 °C.

**Extended Hückel Molecular Orbital (EHMO) Calculations.** Extended Hückel calculations were performed using the CAChe system (version 3.0 for Macintosh).[23] Parameters are given in Table 6. The $[H_3(CO)(I)W]^{2-}$ fragment was used to model the Tp′(CO)(I)W moiety. The molecular geometry was set as follows: the H atoms occupy three facial sites of the octahedron with W−H distances set at 1.70 Å and H−W−H angles of 90°. The W−C bond length was fixed at 1.90 Å, the C−O bond length was set to 1.15 Å, and the W−I bond length was set to 2.80 Å.

**$[H_3(CO)(I)W\{HC{\equiv}CH\}]^{2-}$.** The remaining octahedral site of the $[H_3W(CO)I]^{2-}$ fragment was occupied by HC≡CH in order to model Tp′(CO)(I)W{RC≡CR′}. The alkyne C≡C distance was set at 1.24 Å with the center of the alkyne unit 1.90 Å from tungsten. A bent-acetylene geometry was idealized with H−C≡C angles of 135° and C−H distances of 1.00 Å. The described geometry was frozen, while the acetylene unit was allowed to revolve about the axis defined by W and the center of the alkyne C≡C bond. The energy was calculated at intervals of 5° as the alkyne was rotated 180°.

**$[H_3(CO)(I)W\{HC{\equiv}CCH_2\}]^{3-}$.** The remaining octahedral site of the $[H_3W(CO)I]^{2-}$ fragment was occupied by $[HC{\equiv}CCH_2]^-$ in order to model the anionic intermediate resulting from deprotonation of Tp′(CO)(I)W{RC≡CCH$_2$R′}. The alkyne C≡C distance was set at 1.24 Å with the center of the alkyne unit 1.90 Å from tungsten. A bent-acetylene geometry was idealized with a H−C≡C angle of 135° and C−H distances of 1.00 Å. The C≡C−C angle was fixed at 139° with the C−C bond length set at 1.34 Å, a typical C−C double-bond length. The atoms of the $CH_2$ unit lie in the plane of the rest of the alkyne unit with C−H bond lengths of 1.10 Å and C−C−H angles of 121°. The described geometry was frozen, while the deprotonated acetylene unit was allowed to revolve about the axis defined by W and the center of the alkyne C≡C bond. The energy was calculated at intervals of 5° as the alkyne was rotated by a total of 360°. In addition, with the $[HC{\equiv}CCH_2]^-$ aligned parallel to the W−CO bond, the $CH_2$ unit was allowed to rotate about the axis defined by the C−C bond of the alkyne

carbon and the propargyl carbon. The energy was tabulated at intervals of 10° as the $CH_2$ unit rotated 180°.

**X-ray Structures.** For **7**, **11**, and **(+)-14(*SS*)** a single crystal was mounted on a glass wand and coated with epoxy. Experimental parameters for data collection and refinement can be found in Table 1.

**Acknowledgment.** We gratefully acknowledge the National Science Foundation for support of this research.

**Supporting Information Available:** Text giving the complete Experimental Section with IR, NMR, and analytical data and tables of thermal parameters, atomic positions, and all bond distances and angles for **7**, **11**, and **(+)-14(*SS*)**. This material is available free of charge via the Internet at http://pubs.acs.org.

OM020416G